Decline of CSC function may be a major cause of the decrease in regenerative capacity in aging and disease (Rota et al., 2006). Although some of the growth factors involved in *Kit*$^{+}$ CSC proliferation and survival have been identified, factors regulating *Kit*$^{-}$ CSCs have yet to be defined (Gude et al., 2006; Limana et al., 2005; Urbanek et al., 2005a). In this study, we sought to identify single proliferative cells from the adult heart without progenitor selection using particular surface markers. Using this unbiased approach, we have established clonal CSC lines and demonstrated that the majority of the telomerase-active progenitor-cell colonies expressed Sca-1 and showed mesenchymal-cell-like character. We also show that targeting the Sca-1 transcripts in CSCs used for cell grafting leads to failure of their ability to prevent cardiac remodeling after myocardial infarction. The antiapoptotic and angiogenetic paracrine activities of intrinsic Sca-1 signaling in CSCs promote direct CSC proliferation and survival, and contribute to neovascularization in the host myocardium for efficient cardiovascular regeneration.

Results

Clonal isolation of cardiac stem cells in the adult heart

To identify the single entity of CSCs in the adult heart, we employed an unbiased approach using a single-cell clonogenic isolation technique to isolate a proliferative cell population. Singly dissociated GFP-labelled transgenic cells derived from the hearts of GFP transgenic mice were plated at a density of one cell per well in serum-free medium (Fig. 1A,B). Altogether, 11,520 single cells were deposited, and from 9541 single cells determined by inspection on day 1 to be present as one individual cell per well, a total of 11 clones arose within 7 days. Eight out 11 clones failed to grow in serum-free medium after 7 days in culture, and 3 clones (~0.03%) could proliferate to form spherical clusters and were continuously expanded after 14 days (Fig. 1C). The three independent colonies were re-dissociated and re-plated in low-serum for expansion, and individual CSC colonies were used for the following experiments to characterize clonal CSCs.

Characterization of clonally amplified CSCs

Immunophenotyping revealed that the clonal CSCs strongly expressed Sca-1, which is used as a marker to identify cardiac progenitor cells from the adult heart (Matsuura et al., 2004; Oh et al., 2003), whereas KIT-positive cells were rarely detected (Fazel et al., 2006; Gude et al., 2006; Pfister et al., 2005) (Fig. 1D). Notably, CSCs did not express the hematopoietic and endothelial progenitor-cell-specific surface antigens CD45, CD34 and CD31, but did express the typical mesenchymal stem-cell surface antigens CD90, CD105, CD29, CD44, CD106, CD73 and CD13 (Pittenger and Martin, 2004). The three individual CSCs exhibited an identical immunophenotyping for the surface marker analysis. The cell membrane antigens Sca-1, KIT, CD45, and CD34 were not destroyed by collagenase treatment as tested in bone marrow (data not shown).

Gene expression was then examined in CSC clones using reverse transcriptase (RT)-PCR (Fig. 1E). Three individual colonies were analyzed and most of the clones expressed Bcrp1, polycomb group protein Bmi1 and also telomerase reverse transcriptase (TERT), which has been reported to be absent in cardiac fibroblasts (Leri et al., 2001). Although Nanog was detectable in all of the colonies examined, none of the colonies – unlike embryonic stem (ES) cells – were positive for OCT4 or UTF1. Some but not all of the colonies expressed HNF3β, brachyury and SOX2, which are endodermal, mesodermal and ectodermal precursor markers, respectively. These results distinguished clonal CSCs from mouse fibroblasts, which are negative for all of the ES cell markers described above (Takahashi and Yamanaka, 2006). In addition, all of the colonies analyzed expressed nestin, a marker of immature neural progenitor cells (Joannides et al., 2004).

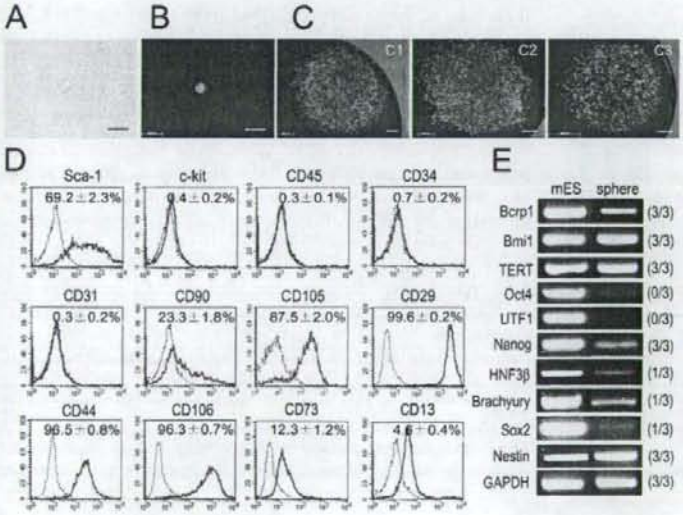

Fig. 1. Clonal isolation and characterization of stem cells in the adult heart. (A,B) Single-cell deposition analysis was performed by the limiting dilution technique. At day 1 of the culture period, wells were inspected for the presence of single cells by phase contrast (A) and GFP fluorescence (B). (C) Colony formation from single cells in 96-well plates at 14 days of culture in serum-free medium. Three-independent colonies derived from single cells are shown. (D) FACS analysis of CSCs. Black line, control IgG; red line, corresponding antibody. Data are representative of three independent clonal CSCs. (E) RT-PCR for CSC clones. The numbers on the right indicate the number of individual colonies that expressed the corresponding genes out of the colonies examined. mES, mouse ES cells used as positive control. Data are representative of three independent clonal CSCs. Bars, 20 μm in A,B; 500 μm in C.

TERT-expressing cells in postnatal heart are associated with Sca-1 expression

TERT has been identified as a key factor controlling telomerase activity, telomere length, and cell growth (Blackburn, 2001). We measured the telomerase activity in clonal CSCs. The three individual CSCs displayed significantly elevated telomerase activity (Fig. 2A). To directly characterize TERT-expressing cells in the adult heart, we engineered transgenic mice expressing enhanced green fluorescent protein (EGFP) under the control of the mouse *Tert* promoter (Fig. 2B). We identified two transgenic founders by genomic DNA screening and established two independent lines (Fig. 2C). In order to examine the efficacy of mouse *Tert* promoter in the heart in vivo, cells isolated from transgenic hearts were sorted by EGFP signal and the EGFP-positive cells were found to be TERT-expressing cells, which were not detectable in EGFP$^-$ populations (Fig. 2D). As expected from high telomerase activities of clonal CSCs shown in Fig. 2A, three individual CSC clones showed TERT expression (Fig. 2D). To further characterize the TERT-positive cells in the heart, FACS analysis was performed. FACS of the cells prepared from the heart of adult mice expressing TERT-EGFP indicated that TERT^{GFP}-positive cells constitute a population that is positive for Sca-1 but rarely expressing detectable levels of c-kit, CD45, CD34, or CD31 (Fig. 2E).

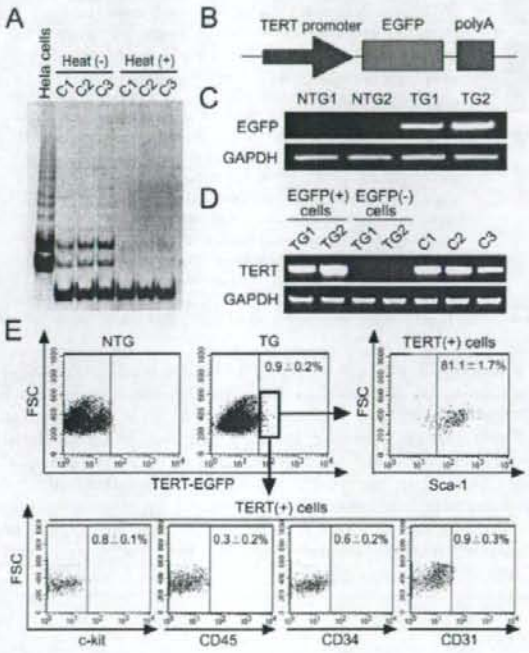

Fig. 2. TERT-expressing cells in adult heart are associated with Sca-1 expression. (A) Telomerase activity was measured by the TRAP assay in three independent clonal-CSCs. The cells were treated with or without heat and used as templates. Hela cells were used as positive controls. (B) Construction of EGFP transgene under the control of the TERT promoter. (C) PCR of genomic DNA from 2 independent TERT-EGFP transgenic lines and respective NTG littermate controls. (D) The expression of TERT on EGFP-positive and EGFP-negative cells sorted from TERT-EGFP transgenic hearts is shown by RT-PCR. The TERT expression was detectable in all three independent clonal CSCs shown in Fig. 1C. (E) FACS analysis of the primary EGFP-positive cells isolated from TERT-EGFP mice (TG). Expression of Sca-1, KIT, CD45, CD34, and CD31 in EGFP-positive cells was examined. Cells from NTG littermates were used as negative control. Data are representative of six independent experiments.

Generation of Sca-1 knockdown (KD) mice

To functionally characterize clonal CSCs, majority of which could be marked by Sca-1 expression, we generated Sca-1 KD mice in which double-stranded (ds)-Sca-1 RNA was expressed under the control of an RNA polymerase II promoter (Fig. 3A) (Shinagawa and Ishii, 2003). The vector pDECAP-Sca-1 expressing ds-Sca-1 RNA with a small loop for transcript pausing and full-length Sca-1 were co-transfected into HEK 293 cells at various concentrations, and the reduction in Sca-1 expression was examined by both RT-PCR and FACS (Fig. 3B,C). Two lines of Sca-1 KD mice were obtained, in which endogenous Sca-1 protein levels (Fig. 3D) in the heart were apparently reduced.

Targeting Sca-1 transcripts affects proliferation and survival but not differentiation of CSCs

To test the function of Sca-1 in CSC development, we examined the ability to clonally proliferate in vitro of single cells from the adult heart of Sca-1 KD and non-transgenic (NTG) littermate mice using a single-cell deposition analysis. This revealed that the percentage of colony-forming cells from Sca-1 KD hearts was significantly lower than that from NTG hearts (Sca-1 KD ~0.007% vs NTG ~0.03%, Fig. 3E). We isolated 11 clones from NTG hearts and four clones from Sca-1 KD hearts, of which eight NTG- and two Sca-1 KD-clones exhibited features of mesenchymal phenotype (data not shown), showed Nanog and Bcrp1 expression by RT-PCR, and could proliferate for more than 14 days (Fig. 3F). Of the clones obtained, four clones expressed brachyury, which is a primitive streak marker (Gadue et al., 2006). Sca-1 expression in CSCs isolated from Sca-1 KD mice was markedly inhibited compared with NTG controls (Fig. 3G). Therefore, we investigated whether Sca-1 expression affects the replicative growth of clonal CSCs in independent cell-culture (Fig. 3H). As shown in Fig. 3I, Sca-1 KD CSCs showed significantly impaired growth kinetics compared with those of NTG CSCs. We determined the molecular mechanisms by which Sca-1 KD mice showed retarded CSC growth. As shown in Fig. 3J, BrdU incorporation and phosphorylation of histone H3 were clearly reduced in the Sca-1 KD CSCs compared with NTG controls, whereas p53 expression levels were significantly increased in the Sca-1 KD CSCs. Telomerase activities were also significantly impaired in the Sca-1 KD CSCs (Fig. 3K).

Of the CSC clones isolated, clones 2, 3 and 6 from NTG and clone 1 from Sca-1 KD mice, all of which expressed brachyury, were chosen for subsequent series of experiments. We asked whether the decrease in clonal CSC growth mediated by Sca-1 KD is associated with an increase in apoptosis. CSCs were isolated from the hearts of NTG and Sca-1 KD mice and were incubated with 100 and 200 μM H_2O_2 for 18 hours, and the surviving cells were analyzed by TUNEL staining. As shown

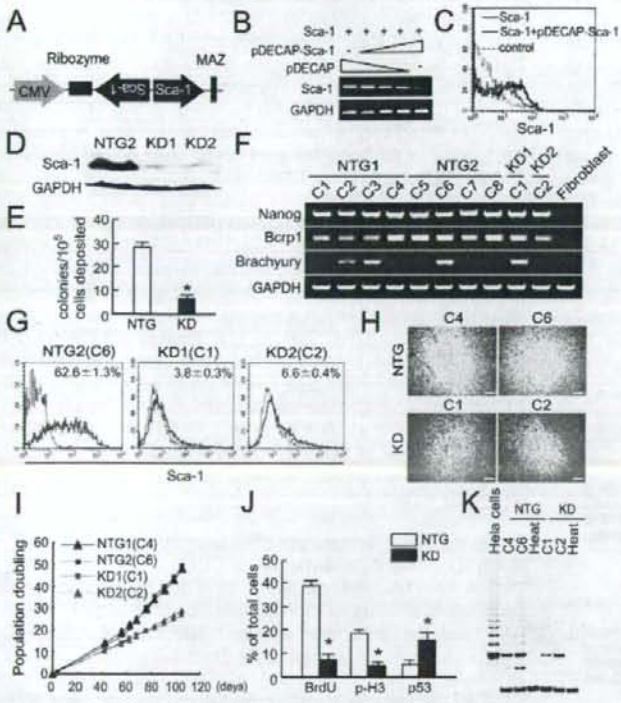

Fig. 3. Generation of Sca-1 KD mice. (A) Construction of the pDECAP-Sca-1 vector. (B,C) Decrease in exogenous Sca-1 expression induced by pDECAP-Sca-1 as shown by RT-PCR (B) and FACS (C) in HEK 293 cells. The total amount (8 μg) of plasmids co-transfected was the same in each experiment (n=3). (D) Decrease in Sca-1 protein levels in the hearts from two independent Sca-1 KD lines. (E) The frequency of CSC colonies from NTG- and Sca-1 KD hearts is shown. Data are expressed as the mean number of colonies formed per 10^5 single cells deposited ± s.e. (n=4). *P<0.01 vs NTG. (F) RT-PCR for embryonic and mesodermal precursor markers. Cardiac fibroblasts were used as negative control. (G) Decrease in Sca-1 expression from two independent Sca-1 KD CSCs clones. Black line, control IgG; red line, Sca-1. (H) Phase-contrast images of respective CSC clones at 14 days of culture in serum-free medium. Bars, 500 μm. (I) Growth kinetics of two independent clonal CSCs isolated from NTG (black lines, C4 and C6) and Sca-1 KD (red lines, C1 and C2) mice. (J) BrdU incorporation, phosphorylated histone-H3 (p-H3) and p53 expression from five independent experiments are shown. *P<0.01 vs NTG. (K) Loss of telomerase activity in the clonal CSCs (C1 and C2) isolated from two independent lines of Sca-1 KD mice.

in Fig. 4A, H_2O_2 induced apoptosis in a dose-dependent manner, and the extent of apoptosis was significantly higher in CSCs isolated from Sca-1 KD hearts than that in NTG-CSCs.

Activation of EGF and bFGF signaling in endothelial cells leads to the phosphorylation of a number of downstream effectors, including Akt and MAPKs (Sulpice et al., 2002). To test the role of these kinases in Sca-1-mediated CSC growth, the activation of Akt and MAPKs in response to EGF and bFGF was examined (Fig. 4B). Incubation of CSCs with EGF and bFGF resulted in a rapid enhancement of Akt, ERK1/2, and JNK1/2, but not in phosphorylation of p38. Although activation of Akt could be abolished by inhibition of Sca-1 transcripts, phosphorylation of three MAPKs was unaffected. These results raise the issue of whether Sca-1-mediated signaling regulates CSC differentiation in vitro. The potential of CSCs to give rise to cardiovascular lineages was not affected by targeting Sca-1 transcripts – as shown by immunostaining (Fig. 5A) and by RT-PCR to assess gene profiles typical of cardiac muscle, smooth muscle and endothelial cell differentiation after specific inductions for 14 days (Fig. 5B),

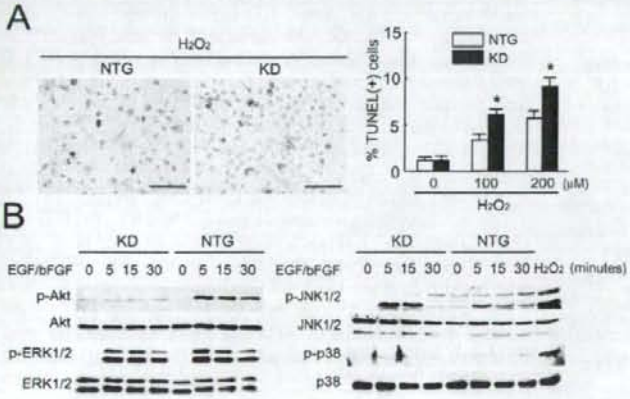

Fig. 4. Sca-1-mediated signaling activates Akt to support CSC proliferation and survival. (A) Representative photographs of TUNEL assay obtained from NTG- or Sca-1 KD-derived CSCs treated with 200 μM H_2O_2 for 18 hours. The numbers of apoptotic cells (brown nuclei) in NTG (C6)- or Sca-1 KD-CSCs (C1) are shown (n=8). *P<0.01 versus NTG. (B) Loss of Sca-1 diminished EGF and bFGF-induced Akt activation in CSCs. CSCs treated with 200 μm H_2O_2 for 15 minutes were used as positive controls. Bars, 50 μm in A.

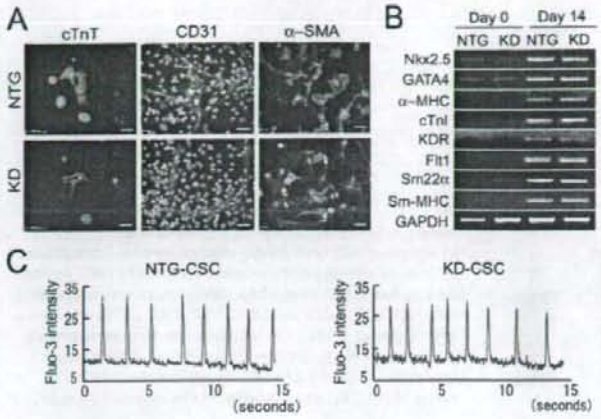

Fig. 5. Loss of Sca-1 transcripts does not affect the differentiation potential of clonal CSCs. (A) Differentiation of NTG-derived or Sca-1 KD-derived clonal CSCs. Cardiac muscle cell (cardiac troponin-T), endothelial cell (CD31) and vascular smooth muscle cell (α-SMA) differentiation were 1.24±0.3%, 12.4±1.8% and 31.9±2.5%, respectively, for NTG-CSCs (C2, C3 and C6, respectively), and 1.23±0.3%, 12.1±2.1% and 32.2±4.7%, respectively, for Sca-1 KD-CSCs (C1). Nuclei are stained by DAPI (blue). Bars, 20 μm in A. (B) RT-PCR showed that the differentiation potential into the three different lineages were similar for both types of CSCs (n=3). (C) Representative Ca^{2+} transient in beating cardiomyocytes. Clone 2, 3 and 6 from NTG and clone 1 from Sca-1 KD mice, all expressed brachyury at baseline, were used for analysis. Intensities were corrected by background amplitude and expressed as arbitrary units (n=3).

and a study investigating the Ca^{2+} transient in beating cardiomyocytes (Fig. 5C).

Loss of Sca-1 transcripts in CSCs fails to improve cardiac function due to diminished donor-cell proliferation, survival and engraftment after cell transplantation

The data described above support the hypothesis that loss of Sca-1 results in a retarded regenerative capacity of CSCs in vivo. To further examine this possibility, we performed cell transfer experiments into ischemic myocardium. 5×10^5 CSCs that had been clonally isolated and expanded from the hearts of Sca-1 KD (C1) and NTG (C6) mice were transplanted into wild-type (WT) mice 1 hour after myocardial infarction. Cardiac MRI was performed 4 weeks after cell grafting and showed that transplantation of Sca-1-KD CSCs resulted in significantly larger left ventricular volume and an increased infarct rate as compared with NTG-CSC implantation (Fig. 6A,B).

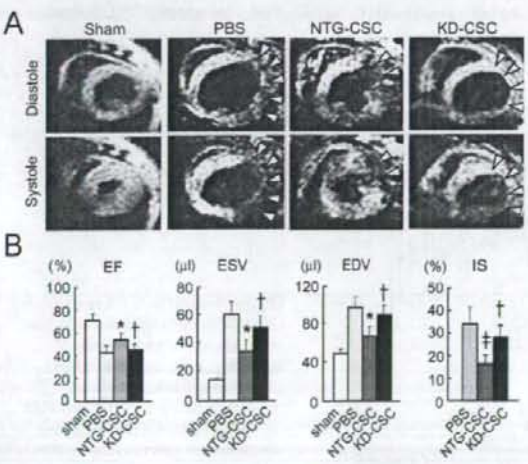

Fig. 6. Sca-1 KD CSC transplantation fails to prevent cardiac remodeling after myocardial infarction. (A,B) WT mice received transplantation of either NTG- or Sca-1 KD mice-derived CSCs 1 hour after infarction. Cardiac MRI was performed 4 weeks after CSC transplantation (n=8). Arrowheads indicate akinetic regions. White bars, sham-operated. Myocardial infarction with PBS injection (light gray bars), NTG-CSC (C6, dark gray bars) or Sca-1 KD-CSC (C1, black bars) transplantation are shown. *P<0.05 vs PBS; †P<0.05 versus NTG-CSC; ‡P<0.01 versus PBS injection. EF, ejection fraction; ESV, end-systolic volume; EDV, end-diastolic volume; IS, infarcted size.

We examined the in-vivo effects of Sca-1-mediated CSC regulation we observed in vitro. At day 3 after CSC transplantation into ischemic myocardium, Sca-1 KD CSCs showed significantly fewer engraftments than NTG-CSCs, as verified by measurement of *lacZ* activity (Fig. 7A). This observation was confirmed by the lower Ki67 expression in Sca-1 KD CSCs, indicating that the proliferative potential was significantly impaired in Sca-1 KD CSCs (Fig. 7A). To assess whether Sca-1-mediated control of CSC survival may also be applied to the process of donor-cell engraftment, we analyzed the viability of grafted CSCs, labeled by β-galactosidase (β-gal) staining, on day 3 after the cell grafting. As shown in Fig. 7B, grafted Sca-1 KD CSCs in the ischemic myocardium resulted in more apoptotic cells than NTG-CSCs, suggesting that the transplanted Sca-1 KD CSCs were also susceptible to cell death in vivo.

To further test whether these effects of Sca-1 during the early phase of CSC transplantation may contribute to the early CSC-engraftment and late regeneration process of cardiovascular-lineage cells, we investigated the presence of *lacZ*$^+$ donor cells at day 7 and characterized their individual phenotypes 4 weeks after transplantation. As shown in Fig. 8A, the frequency of *lacZ*$^+$ cells observed 7 days post cell transfer was significantly lower in Sca-1 KD CSC grafts compared with NTG-CSC transplantation, resulting in substantially insufficient cardiovascular regeneration within the ischemic regions 4 weeks after CSC transplantation (Fig. 8B-D).

Sca-1 KD CSC transplantation fails to prevent myocardial apoptosis and limits angiogenesis, partially due to the failure of paracrine effector secretion

Last, we assessed whether the loss of Sca-1 in transplanted

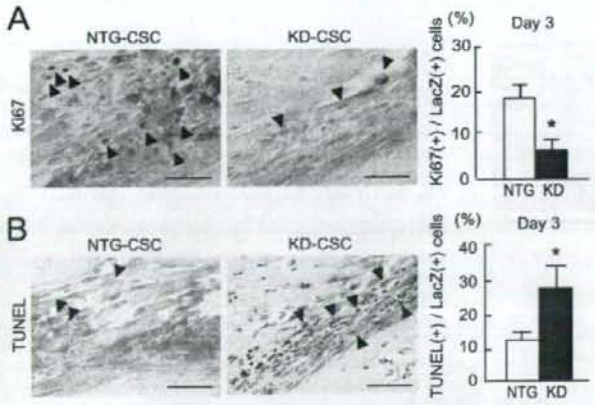

Fig. 7. Sca-1 transcripts are required for CSC proliferation and survival in vivo. (A) Immunohistochemistry of transplanted *lacZ*$^+$ cells 3 days after infarction. Transplanted *lacZ*$^+$ cells entering cell cycle were detected as Ki67-positive cells (arrowheads) (n=6). Myocardial infarction transplanted with NTG-CSCs (C6) and Sca-1 KD CSCs (C1) are shown. *P<0.01 versus NTG. (B) Apoptotic features (arrowheads, brown nuclei) of *lacZ*$^+$ engrafted cells are shown at day 3 after NTG- or Sca-1 KD-CSC transplantation. *P<0.01 versus NTG-CSC transplantation (n=6). Bars, 50 μm in A,B.

CSCs affects myocardial apoptosis and angiogenesis. At day 3, transplantation of Sca-1 KD CSCs resulted in a high level of myocardial apoptosis in the ungrafted area of the infarcted border zone, whereas fewer TUNEL-positive cells were observed in NTG-CSC-injected hearts (Fig. 9A). Furthermore, transplantation of Sca-1 KD CSCs failed to improve capillary density 2 weeks after infarction in the ischemic region as compared with NTG-CSC injection (Fig. 9B). To explore the molecular mechanisms of Sca-1-mediated myocardial apoptosis and neoangiogenesis, we then oxygen-starved CSCs for 8 hours and measured the levels of mRNA for secreted paracrine factors by RT-PCR. As shown in Fig. 9C, downregulation of hepatocyte growth factor (HGF) in Sca-1 KD CSCs was evident at baseline normoxia. After hypoxia, a greater increase in the expression of VEGF and HGF was observed in NTG-CSCs compared with that in Sca-1 KD CSCs. The expression pattern of insulin-like growth factor-1 (IGF1) under normoxic and hypoxic conditions was comparable in CSCs from NTG and Sca-1 KD hearts.

Discussion

Recent reports have shown that clonogenic CSCs reside in

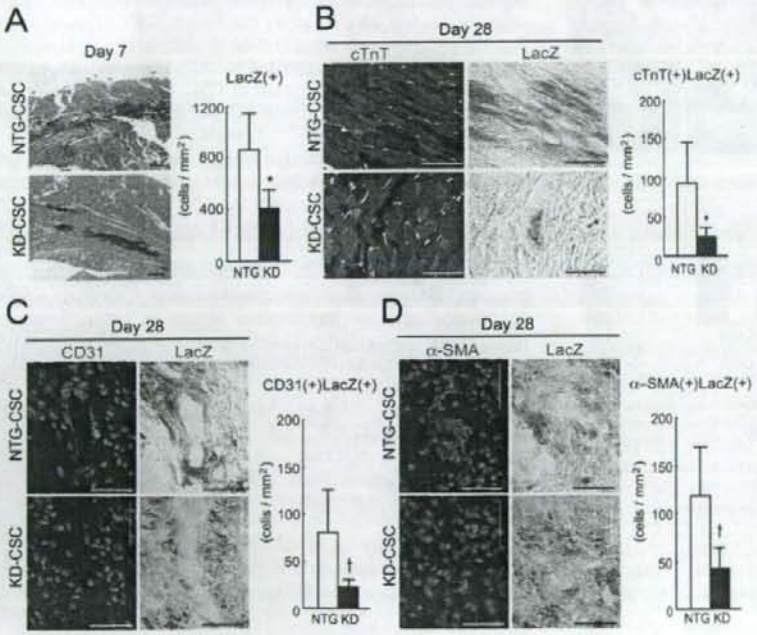

Fig. 8. Loss of Sca-1 transcripts in clonal CSC transplantation shows less donor-cell engraftment, resulting in the decrease in late cardiovascular regeneration. (A) Engrafted *lacZ*$^+$ cells in NTG (C6)- and Sca-1 KD-CSC (C1)-transplanted hearts at day 7 after infarction. Sections were counterstained using H&E. (B-D) The representative images and frequencies of cardiomyocytes (cardiac troponin-T, red), and endothelial (CD31) and smooth muscle cells (α-SMA) in *lacZ*$^+$ cells at day 28 are shown (n=6). Note that differentiated *lacZ*$^+$ cardiomyocytes co-express connexin-43 (yellow). Bars, 100 μm in A; 20 μm in B; 50 μm in C,D.

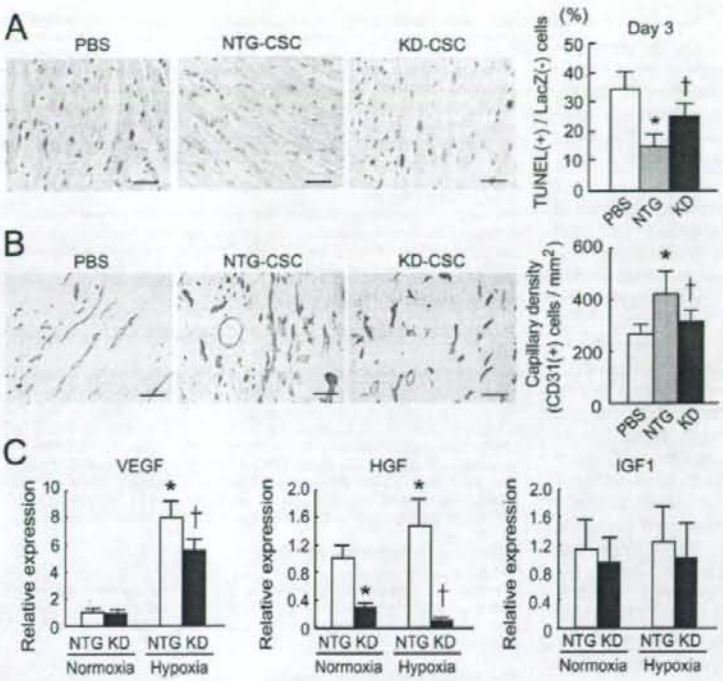

Fig. 9. Transplantation of Sca-1 KD CSCs fails to prevent myocardial apoptosis and limits neoangiogenesis after myocardial infarction partially due to the failure of paracrine effector secretion. (A) TUNEL staining revealed the apoptotic cardiomyocytes in the border zone of PBS-treated, NTG (C6)- and Sca-1 KD-CSC (C1)-transplanted hearts at day 3; (n=6). *P<0.01 vs PBS. †P<0.01 vs NTG. (B) Capillary density of infarcted border zone of transplanted hearts at day 14 after myocardial infarction. Capillary density was measured by staining of CD31 (brown) and corrected by the area analyzed. (n=8). *P<0.01 vs PBS-treated mice; †P<0.01 vs NTG-CSC-transplanted mice. Bars, 50 μm in A,B. (C) Relative mRNA expression levels of VEGF, HGF, and IGF1 normalized by 18S expression in NTG- and Sca-1 KD-CSCs under normoxic and hypoxic conditions (n=7). *P<0.01 vs NTG-CSCs under normoxia; †P<0.01 vs NTG-CSCs under hypoxia.

mammalian hearts, judging on the basis of specific cell-surface markers which are also expressed by hematopoietic and endothelial progenitor cells (Beltrami et al., 2003; Linke et al., 2005). Using an unbiased approach, our study has demonstrated that clonally proliferated CSCs express Sca-1 with ES cell-like and mesenchymal-cell-like characteristics, and are associated with TERT expression.

Our results, showing low expression of KIT in clonal *Kit*$^+$ CSCs, differ from the findings of some previous studies (Linke et al., 2005; Messina et al., 2004) but are consistent with those of recent reports about the adult heart (Fazel et al., 2006; Gude et al., 2006; Matsuura et al., 2004; Oh et al., 2003; Pfister et al., 2005; Tateishi et al., 2007). The reasons for this discrepancy are unclear. However, retrospective analysis data that directly sorted TERT-expressing cells from TERT-EGFP hearts (that were genetically isolated without the modification by cell culture) have shown that the majority of heart-resident TERT-positive cells could be identified via the expression of Sca-1. This implies that our findings were neither the result of intra-clonal variability nor due to contamination by cardiac fibroblasts during cell expansion. Recent report demonstrated that the expression levels of Sca-1 and KIT appear to be changed during myocardial maturation in ES cells (Wu et al., 2006).

Mesenchymal stem cells have been isolated from many tissues, including human heart (da Silva Meirelles et al., 2006; Tateishi et al., 2007). It is notable that CSCs expressed general characteristics of mesenchymal stem cells according to the analysis of cell-surface markers and partially showed the embryonic factors, as previously reported in clonal amniotic fluid-derived mesenchymal stem cells (Tsai et al., 2006). These observations indicated that the epithelial-mesenchymal transition (EMT) may occur in adult CSCs to produce proliferative precursors, which may undergo a reversible commitment into the directions of either mesenchymal or cardiac lineage, depending on the inductive conditions (Wessels and Perez-Pomares, 2004). Several reports suggest that the source of CSCs may include the neural crest (Tomita et al., 2005), primitive epicardial cells (Hay, 2005) or perivascular cells (da Silva Meirelles et al., 2006) through the EMT.

Regulating stem cell self-renewal is an essential feature of the niche where stem cells must be exposed to sufficient intrinsic-factors to maintain the proper stem cell number for the demands of tissue repair. We focused on Sca-1-mediated regulation in CSCs for the first time and found that normal Sca-1 function is associated with CSC proliferation and survival, contributing to early donor-cell engraftment and late cardiovascular differentiation, which is consistent with the prevailing view of the role of Sca-1 in the ability of hematopoietic stem cells and bone-marrow-derived mesenchymal stem cells to self-replicate (Bonyadi et al., 2003; Ito et al., 2003). Although the function of Sca-1 in skeletal muscle progenitors was not consistent with our observations in CSCs, the cell fate decision might be cell-type specific and/or age dependent (Mitchell et al., 2005). The mode of action of *Lin*$^-$*-Kit*$^+$ cells in the heart or bone marrow has been intensively investigated in gain- (Dawn et al., 2006; Urbanek et al., 2005a)

and loss-of-function experiments, and the function of these cells was validated by bone marrow reconstitution studies to completely rescue the defective cardiac repair in c-kit mutant mice after infarction (Ayach et al., 2006; Fazel et al., 2006), consistent with the lack of cardiac decompensation after pressure-overload in c-kit mutant mice (Hara et al., 2002) and our present observation indicating the rarity of c-kit$^+$ cells in TERT-expressing CSCs.

Sca-1 was originally identified as an antigen upregulated in activated lymphocytes, and was shown to be linked to the lipid bilayer as a glycosyl phosphatidylinositol (PtdIns)-anchored protein that activates cell signaling via mediators such as Akt (Reiser et al., 1986). The proliferation of CSCs appears to be dependent on the capacity of the cells to undergo cell cycle progression through the phosphorylation of Akt in response to EGF and bFGF stimulation, as observed in neural stem cells (Groszer et al., 2006). Our observations are supported by two independent gain-of-function studies demonstrating that the nuclear-targeting of Akt leads to the rapid expansion of comparatively rare *Kit*$^+$ CSCs in the postnatal heart (Gude et al., 2006), and ex-vivo transduction of Akt to bone marrow-derived MSCs can functionally repair the ischemic myocardium through the upregulation of secreted paracrine effectors (Gnecchi et al., 2006; Jiang et al., 2006). Consistent with these studies, our present study also demonstrated that the functional improvement of damaged myocardium after CSCs transplantation was attenuated by Sca-1 KD, in which new vessel formation and inhibition of myocardial apoptosis by release of angiogenic growth factors and myocyte regeneration by grafted CSCs were severely impaired.

Taken together, our results suggest that Sca-1 is expressed in the majority of intrinsic CSCs in the adult heart, which have characteristics of ES-like and mesenchymal-like cells, and implicate the role of Sca-1 in CSC maintenance and function. Sca-1-mediated signaling is important in CSC development in normal circumstances and its beneficial effect might be involved the responses to hypoxic and ischemic conditions. The cardioprotective effect of CSC transplantation that we have shown here indicates that Sca-1-mediated ligand responses may participate in the production of angiogenic and antiapoptotic paracrine effectors, consistent with recent observations demonstrating that induction of VEGF and HGF activates bone marrow-derived mesenchymal stem cells through PI 3-kinase–Akt pathway (Forte et al., 2006; Okuyama et al., 2006). It will be of interest to assess the gene expression profile in CSCs by targeting Sca-1 transcripts to identify the factors responsible for optimizing CSC therapy in heart failure.

Materials and Methods

Clonal isolation and culture of CSCs

Hearts from 6-week-old to-12-week-old GFP transgenic mice (provided by M. Okabe, Osaka University Medical School) (Okabe et al., 1997), Sca-1 KD mice or NTG mice were excised and were perfused with cold PBS to remove the blood cells. The tissues were washed twice, and aortic and pulmonary vessels were removed from the hearts. The dissected hearts were minced, and digested twice for 20 minutes at 37°C with 0.2% type II collagenase and 0.01% DNAse I (Worthington Biochemical Corp, NJ). The cells were passed through a 40-μm filter to remove the debris and were plated into 25-cm^2 dishes in DMEM (Invitrogen) for 30 minutes to allow fibroblasts to adhere. The non-adherent cells were collected and size-fractionated with a 30-70% Percoll gradient to obtain single-cell suspensions by removal of mature cardiomyocytes. For clonal analysis, the resulting cell suspensions were plated in 96-well plates at 1 cell per 100 μl by the limiting dilution technique (Yoon et al., 2005) with serum-free growth medium: DMEM/F12 containing B27 supplement, 20 ng/ml EGF (Sigma), and 40 ng/ml bFGF (Promega). Wells were visually inspected 24 hours after plating to exclude those containing more than one cell per well; then, clones derived from a single cell were further cultivated. On day 14, clonally expanded CSCs from single cells were cultured in low-serum medium consisting of growth medium supplemented with 1×B27 supplement, 2% FBS, and 10 ng/ml leukemia inhibitory factor (CHEMICON). At 60-70% confluence, cells from individual clones were serially reseeded in six-well plates, 25-cm^2, 75-cm^2 and 175-cm^2 flasks for further expansion. Hypoxic conditions were created by incubating cells at 37°C in a CO_2 multi-gas incubator (ASTEC) with an atmosphere of 5% CO_2 and 95% N_2 for 8 hours.

CSC differentiation

For cardiac differentiation analysis, single-cell-derived CSCs were cultured in differentiation medium containing 10% FBS, insulin-transferrin-selenium, and 10 nM dexamethasone (Sigma) for 14 days. Differentiation medium consisting of DMEM/F12 supplemented with 10 ng/ml VEGF or 50 ng/ml PDGF-BB (both from R&D Systems) and 10% FBS was used to induce endothelial and smooth muscle cell differentiation for 14 days, respectively.

Construction of targeting vector and generation of transgenic mice

Full-length Sca-1 cDNA was cloned using the following primers: forward: 5′-CTCTGAGGATGGACACTTCT-3′, reverse: 5′-GGTCTGCAGGAGGACTGA-GC-3′. The 404-bp ds-RNA fragment targeting the N-terminus of Sca-1 was selectively amplified and subcloned into the pDECAP vector (Shinagawa and Ishii, 2003). The plasmid encoding EGFP driven by the mouse *Tert* promoter was provided by N. Hole (University of Durham) (Armstrong et al., 2000) and subcloned into the human growth hormone polyadenylation sequence. Each expression cassette was released and microinjected into the pronuclei of fertilized C57BL/6 oocytes. PCR analysis of tail DNA was used to identify founder transgenic mice.

Retroviral transduction of CSCs

To track cells after injection into the infarcted myocardium, CSCs were engineered to express the bacterial *lacZ* reporter gene. This was done by retroviral infection with a vector (pMSCV-LacZ) encoding the *lacZ* gene and a puromycin resistance gene. After selection with puromycin, the transduction efficiency was evaluated by X-gal staining.

FACS analysis and cell sorting

Single-cell suspensions were stained with the following antibodies: phycoerythrin (PE)-conjugated antibodies against Sca-1, KIT, CD45, CD44, CD90, CD31, CD73, CD106, CD34, CD13, CD29, and isotype control IgG (all from BD Biosciences). Allophycocyanin (APC)-conjugated goat anti-rat IgG was used to detect rat anti-mouse CD105 (Southern Biotech). Dead cells were eliminated using propidium iodide (Sigma) and 10,000 to 50,000 events were collected per sample using a FACS Calibur flow cytometer (BD Biosciences). Bone marrow cells were flushed from the tibiae and femurs of 6-week-old to 12-week-old C57BL/6 mice and compared (with or without collagenase and filtration) (Oh et al., 2003). Single-cell suspensions were harvested from TERT-EGFP transgenic and NTG hearts as the method for CSC preparation, and the EGFP-positive cells were analyzed and sorted on BD FACSAria (Becton Dickinson).

RT-PCR and telomerase activity

Total RNA was prepared from cultured cells using TRIzol (Invitrogen) and cDNA was generated with the SuperScript III First-Strand Synthesis System (Invitrogen). PCR reactions were performed with gene-specific primers. Primer sequences are available on request. To evaluate VEGF, HGF, and IGF1 expression, cDNA was subjected to 40 rounds of amplification (ABI PRISM 7700, Applied Biosystems) with Assay-on-Demand™ primer-probes sets (Applied Biosystems). The mRNA levels were expressed relative to an endogenous control (18S RNA) and the fold-increase in the respective groups versus normoxia NTG-CSCs was calculated. Telomerase activity of single-cell-derived CSCs was measured using a TRAP assay kit, TRAPEZE (CHEMICON), as previously described (Oh et al., 2001).

Calcium transient

Cells were washed three times with 1 mM Ca^{2+} Tyrode's solution as previously described (Kaneko et al., 2000), additional 15 minutes incubation with 1 mM Ca^{2+} Tyrode's containing 1 mM probenecid at 37°C was performed to allow hydrolysis of acetoxymethyl esters within the cells. Fluorescence imaging was performed at 24°C using a fixed-stage microscope (BX50WI, Olympus, Japan) equipped with a multi-pinhole-type confocal scanning system (CSU-21, Yokogawa, Japan). Digitized fluorescence signals were analyzed with Image J software.

Western blotting

Whole protein lysates were extracted with lysis buffer: 50 mM Tris-HCl (pH 7.4), 150 mM NaCl, 0.25% sodium deoxycholate, 1 mM EDTA, 1% Nonidet P-40, 1 mM PMSF and protease inhibitor (PIERCE). For phosphorylation of Akt, ERK1/2, JNK1/2 and p38, 1 mM Na_3VO_4 and 1 mM NaF were added. Transferred

membranes were incubated with rat anti-mouse Sca-1 monoclonal antibody (clone D7, BD Biosciences), antibodies against phosphorylated Akt (S473), Akt, phosphorylated ERK1/2 (T202/Y204), ERK1/2, phosphorylated SAPK/JNK (Thr 183/Tyr185), SAPK/JNK, phosphorylated p38 MAPK (Thr180/Tyr182), p38 MAPK (all from Cell Signaling), or mouse monoclonal anti-GAPDH (Chemicon). Horseradish peroxidase (HRP)-conjugated goat anti-rat IgG, HRP-conjugated sheep anti-mouse IgG and HRP-conjugated donkey anti-rabbit IgG (Amersham Biosciences) were used as secondary antibodies.

Sample fixation and X-gal staining

Hearts were fixed in 1% paraformaldehyde, 0.2% glutaraldehyde, and 0.2% Nonidet P-40. X-gal staining was performed with the following reagents: 5 mM $K_4Fe(CN)_6$, 5 mM $K_3Fe(CN)_6$, 2 mM $MgCl_2$, 0.01% sodium deoxycholate, 0.2% Nonidet P-40, and 1 mg/ml X-gal (Invitrogen). After staining, samples were post-fixed with 4% paraformadehyde and embedded in frozen OCT compound or paraffin.

Histology and immunofluorescence

Fixed cells and frozen sections were stained using the following primary antibodies: mouse anti-cardiac troponin-T (Ab1, Neo Markers), rat anti-mouse CD31 (BD Biosciences), Cy3-conjugated anti-α-SMA (Sigma), rabbit anti-p53 (FL-393, Santa Cruz) and rabbit anti-phosphorylated histone H3 (Ser10, Upstate). Secondary antibodies were conjugated to Alexa Fluor 555 or Alexa Fluor 568, and nuclei were visualized using DAPI (Molecular Probes). BrdU incorporation was examined by incubation with 10 μM BrdU for 1 hour using a detection kit (Roche). For Ki67 immunohistochemistry, we used a Vectastain ABC Elite kit (Vector Laboratories). After antigen retrieval using citrate buffer (pH 6.0) and blockage of endogenous peroxidase activity using 0.3% hydrogen peroxide, the sections were incubated with rat anti-mouse Ki67 antibody (DAKO) for 1 hour at room temperature. Then, the sections were treated with biotinylated secondary antibody followed by incubation with avidin horseradish peroxidase complex. Finally, the sections were counterstained with hematoxylin or H&E staining. Capillary density was estimated by CD31 immunostaining with a Vectastain ABC Elite kit. Apoptotic CSCs or cardiomyocytes were evaluated by the TUNEL assay in fixed cells and paraffin-embedded sections with an ApopTag kit (Chemicon). H_2O_2 was purchased from Wako. Images were captured with a BZ-8000 (Keyence, Japan) and IX 71 (Olympus Corporation, Japan).

Myocardial infarction and cell grafting

Ligation of the left anterior descending (LAD) coronary artery was performed in 12-week-old to 24-week-old C57BL/6 mice (Shimizu Laboratory Supplies, Japan) in accordance with the animal care and use guidelines at Kyoto University Hospital. One hour after the LAD ligation, 5×10^5 cells were suspended in 20 μl of PBS and injected into two sites of the infarcted border zone. In the control group, mice were sham-operated by receiving a left thoracotomy without coronary artery ligation.

Cardiac function and infarct size

Cardiac MRI studies were performed using a 7 T MR scanner, Unity Inova (Varian Inc., Palo Alto, CA) with a 25-mm home-built solenoid-type volume coil. Analysis of end-systolic and end-diastolic LV volumes and LV mass was done using an operator-interactive threshold technique, and stroke volume and cardiac output were calculated. All measurements were performed and analyzed by an individual blinded to the animal group. For in vivo determination of infarct size, end-diastolic epicardial and endocardial contours were traced on the MRI short-axis slices; only akinetic and dyskinetic segments were considered to be infarcted areas (Yang et al., 2004).

Statistics

Data are expressed as the mean ± s.e. Two-tailed Student's *t* test was used to compare the clonality of Sca-1 KD- and NTG-CSCs. Comparison of groups in remaining experiments was unpaired analyses using two-tailed Student's *t* test. Significance level was set at $P<0.05$ (StatView).

We thank the following investigators for their kind gifts of mice or plasmids: M. Okabe, N. Hole, S. Ishii and Y. Yoshida, A. Kosugi. We also thank M. Nishikawa for technical assistance. This work was supported by Grants-in-Aid from the Ministry of Education, Culture, Sports, Science and Technology, and by Grants-in-Aid from the Ministry of Health, Labor and Welfare.

References

Armstrong, L., Lako, M., Lincoln, J., Cairns, P. M. and Hole, N. (2000). mTert expression correlates with telomerase activity during the differentiation of murine embryonic stem cells. *Mech. Dev.* **97**, 109-116.

Ayach, B. B., Yoshimitsu, M., Dawood, F., Sun, M., Arab, S., Chen, M., Higuchi, K., Siatskas, C., Lee, P., Lim, H. et al. (2006). Stem cell factor receptor induces progenitor and natural killer cell-mediated cardiac survival and repair after myocardial infarction. *Proc. Natl. Acad. Sci. USA* **103**, 2304-2309.

Beltrami, A. P., Barlucchi, L., Torella, D., Baker, M., Limana, F., Chimenti, S., Kasahara, H., Rota, M., Musso, E., Urbanek, K. et al. (2003). Adult cardiac stem cells are multipotent and support myocardial regeneration. *Cell* **114**, 763-776.

Blackburn, E. H. (2001). Switching and signaling at the telomere. *Cell* **106**, 661-673.

Bonyadi, M., Waldman, S. D., Liu, D., Aubin, J. E., Grynpas, M. D. and Stanford, W. L. (2003). Mesenchymal progenitor self-renewal deficiency leads to age-dependent osteoporosis in Sca-1/Ly-6A null mice. *Proc. Natl. Acad. Sci. USA* **100**, 5840-5845.

da Silva Meirelles, L., Chagastelles, P. C. and Nardi, N. B. (2006). Mesenchymal stem cells reside in virtually all post-natal organs and tissues. *J. Cell Sci.* **119**, 2204-2213.

Dawn, B., Guo, Y., Rezazadeh, A., Huang, Y., Stein, A. B., Hunt, G., Tiwari, S., Varma, J., Gu, Y., Prabhu, S. D. et al. (2006). Postinfarct cytokine therapy regenerates cardiac tissue and improves left ventricular function. *Circ. Res.* **98**, 1098-1105.

Fazel, S., Cimini, M., Chen, L., Li, S., Angoulvant, D., Fedak, P., Verma, S., Weisel, R. D., Keating, A. and Li, R. K. (2006). Cardioprotective c-kit+ cells are from the bone marrow and regulate the myocardial balance of angiogenic cytokines. *J. Clin. Invest.* **116**, 1865-1877.

Forte, G., Minieri, M., Cossa, P., Antenucci, D., Sala, M., Gnocchi, V., Fiaccavento, R., Carotenuto, F., De Vito, P., Baldini, P. M. et al. (2006). Hepatocyte growth factor effects on mesenchymal stem cells: proliferation, migration, and differentiation. *Stem Cells* **24**, 23-33.

Gadue, P., Huber, T. L., Paddison, P. J. and Keller, G. M. (2006). Wnt and TGF-beta signaling are required for the induction of an in vitro model of primitive streak formation using embryonic stem cells. *Proc. Natl. Acad. Sci. USA* **103**, 16806-16811.

Gnecchi, M., He, H., Noiseux, N., Liang, O. D., Zhang, L., Morello, F., Mu, H., Melo, L. G., Pratt, R. E., Ingwall, J. S. et al. (2006). Evidence supporting paracrine hypothesis for Akt-modified mesenchymal stem cell-mediated cardiac protection and functional improvement. *FASEB J.* **20**, 661-669.

Groszer, M., Erickson, R., Scripture-Adams, D. D., Dougherty, J. D., Le Belle, J., Zack, J. A., Geschwind, D. H., Liu, X., Kornblum, H. I. and Wu, H. (2006). PTEN negatively regulates neural stem cell self-renewal by modulating G0-G1 cell cycle entry. *Proc. Natl. Acad. Sci. USA* **103**, 111-116.

Gude, N., Muraski, J., Rubio, M., Kajstura, J., Schaefer, E., Anversa, P. and Sussman, M. A. (2006). Akt promotes increased cardiomyocyte cycling and expansion of the cardiac progenitor cell population. *Circ. Res.* **99**, 381-388.

Hara, M., Ono, K., Hwang, M. W., Iwasaki, A., Okada, M., Nakatani, K., Sasayama, S. and Matsumori, A. (2002). Evidence for a role of mast cells in the evolution to congestive heart failure. *J. Exp. Med.* **195**, 375-381.

Hay, E. D. (2005). The mesenchymal cell, its role in the embryo, and the remarkable signaling mechanisms that create it. *Dev. Dyn.* **233**, 706-720.

Ito, C. Y., Li, C. Y., Bernstein, A., Dick, J. E. and Stanford, W. L. (2003). Hematopoietic stem cell and progenitor defects in Sca-1/Ly-6A-null mice. *Blood* **101**, 517-523.

Jiang, S., Haider, H., Idris, N. M., Salim, A. and Ashraf, M. (2006). Supportive interaction between cell survival signaling and angiocompetent factors enhances donor cell survival and promotes angiomyogenesis for cardiac repair. *Circ. Res.* **99**, 776-784.

Joannides, A., Gaughwin, P., Schwiening, C., Majed, H., Sterling, J., Compston, A. and Chandran, S. (2004). Efficient generation of neural precursors from adult human skin: astrocytes promote neurogenesis from skin-derived stem cells. *Lancet* **364**, 172-178.

Kaneko, T., Tanaka, H., Oyamada, M., Kawata, S. and Takamatsu, T. (2000). Three distinct types of Ca(2+) waves in Langendorff-perfused rat heart revealed by real-time confocal microscopy. *Circ. Res.* **86**, 1093-1099.

Kawada, H., Fujita, J., Kinjo, K., Matsuzaki, Y., Tsuma, M., Miyatake, H., Muguruma, Y., Tsuboi, K., Itabashi, Y., Ikeda, Y. et al. (2004). Nonhematopoietic mesenchymal stem cells can be mobilized and differentiate into cardiomyocytes after myocardial infarction. *Blood* **104**, 3581-3587.

Laugwitz, K. L., Moretti, A., Lam, J., Gruber, P., Chen, Y., Woodard, S., Lin, L. Z., Cai, C. L., Lu, M. M., Reth, M. et al. (2005). Postnatal isl1+ cardioblasts enter fully differentiated cardiomyocyte lineages. *Nature* **433**, 647-653.

Leri, A., Barlucchi, L., Limana, F., Deptala, A., Darzynkiewicz, Z., Hintze, T. H., Kajstura, J., Nadal-Ginard, B. and Anversa, P. (2001). Telomerase expression and activity are coupled with myocyte proliferation and preservation of telomeric length in the failing heart. *Proc. Natl. Acad. Sci. USA* **98**, 8626-8631.

Limana, F., Germani, A., Zacheo, A., Kajstura, J., Di Carlo, A., Borsellino, G., Leoni, O., Palumbo, R., Battistini, L., Rastaldo, R. et al. (2005). Exogenous high-mobility group box 1 protein induces myocardial regeneration after infarction via enhanced cardiac C-kit+ cell proliferation and differentiation. *Circ. Res.* **97**, e73-e83.

Linke, A., Muller, P., Nurzynska, D., Casarsa, C., Torella, D., Nascimbene, A., Castaldo, C., Cascapera, S., Bohm, M., Quaini, F. et al. (2005). Stem cells in the dog heart are self-renewing, clonogenic, and multipotent and regenerate infarcted myocardium, improving cardiac function. *Proc. Natl. Acad. Sci. USA* **102**, 8966-8971.

Matsuura, K., Nagai, T., Nishigaki, N., Oyama, T., Nishi, J., Wada, H., Sano, M., Toko, H., Akazawa, H., Sato, T. et al. (2004). Adult cardiac Sca-1-positive cells differentiate into beating cardiomyocytes. *J. Biol. Chem.* **279**, 11384-11391.

Messina, E., De Angelis, L., Frati, G., Morrone, S., Chimenti, S., Fiordaliso, F., Salio, M., Battaglia, M., Latronico, M. V., Coletta, M. et al. (2004). Isolation and expansion of adult cardiac stem cells from human and murine heart. *Circ. Res.* **95**, 911-921.

Mitchell, P. O., Mills, T., O'Connor, R. S., Graubert, T., Dzierzak, E. and Pavlath, G. K. (2005). Sca-1 negatively regulates proliferation and differentiation of muscle cells. *Dev. Biol.* **283**, 240-252.

Moretti, A., Caron, L., Nakano, A., Lam, J. T., Bernshausen, A., Chen, Y., Qyang, Y., Bu, L., Sasaki, M., Martin-Puig, S. et al. (2006). Multipotent embryonic Isl1(+)

progenitor cells lead to cardiac, smooth muscle, and endothelial cell diversification. *Cell* **127**, 1151-1165.

Murry, C. E., Soonpaa, M. H., Reinecke, H., Nakajima, H., Nakajima, H. O., Rubart, M., Pasumarthi, K. B., Virag, J. I., Bartelmez, S. H., Poppa, V. et al. (2004). Haematopoietic stem cells do not transdifferentiate into cardiac myocytes in myocardial infarcts. *Nature* **428**, 664-668.

Oh, H., Taffet, G. E., Youker, K. A., Entman, M. L., Overbeek, P. A., Michael, L. H. and Schneider, M. D. (2001). Telomerase reverse transcriptase promotes cardiac muscle cell proliferation, hypertrophy, and survival. *Proc. Natl. Acad. Sci. USA* **98**, 10308-10313.

Oh, H., Bradfute, S. B., Gallardo, T. D., Nakamura, T., Gaussin, V., Mishina, Y., Pocius, J., Michael, L. H., Behringer, R. R., Garry, D. J. et al. (2003). Cardiac progenitor cells from adult myocardium: homing, differentiation, and fusion after infarction. *Proc. Natl. Acad. Sci. USA* **100**, 12313-12318.

Okabe, M., Ikawa, M., Kominami, K., Nakanishi, T. and Nishimune, Y. (1997). 'Green mice' as a source of ubiquitous green cells. *FEBS Lett.* **407**, 313-319.

Okuyama, H., Krishnamachary, B., Zhou, Y. F., Nagasawa, H., Bosch-Marce, M. and Semenza, G. L. (2006). Expression of vascular endothelial growth factor receptor 1 in bone marrow-derived mesenchymal cells is dependent on hypoxia-inducible factor 1. *J. Biol. Chem.* **281**, 15554-15563.

Orlic, D., Kajstura, J., Chimenti, S., Jakoniuk, I., Anderson, S. M., Li, B., Pickel, J., McKay, R., Nadal-Ginard, B., Bodine, D. M. et al. (2001). Bone marrow cells regenerate infarcted myocardium. *Nature* **410**, 701-705.

Pfister, O., Mouquet, F., Jain, M., Summer, R., Helmes, M., Fine, A., Colucci, W. S. and Liao, R. (2005). CD31– but not CD31+ cardiac side population cells exhibit functional cardiomyogenic differentiation. *Circ. Res.* **97**, 52-61.

Pittenger, M. F. and Martin, B. J. (2004). Mesenchymal stem cells and their potential as cardiac therapeutics. *Circ. Res.* **95**, 9-20.

Reiser, H., Oettgen, H., Yeh, E. T., Terhorst, C., Low, M. G., Benacerraf, B. and Rock, K. L. (1986). Structural characterization of the TAP molecule: a phosphatidylinositol-linked glycoprotein distinct from the T cell receptor/T3 complex and Thy-1. *Cell* **47**, 365-370.

Rota, M., LeCapitaine, N., Hosoda, T., Boni, A., De Angelis, A., Padin-Iruegas, M. E., Esposito, G., Vitale, S., Urbanek, K., Casarsa, C. et al. (2006). Diabetes promotes cardiac stem cell aging and heart failure, which are prevented by deletion of the p66shc gene. *Circ. Res.* **99**, 42-52.

Shinagawa, T. and Ishii, S. (2003). Generation of Ski-knockdown mice by expressing a long double-strand RNA from an RNA polymerase II promoter. *Genes Dev.* **17**, 1340-1345.

Sulpice, E., Bryckaert, M., Lacour, J., Contreres, J. O. and Tobelem, G. (2002). Platelet factor 4 inhibits FGF2-induced endothelial cell proliferation via the extracellular signal-regulated kinase pathway but not by the phosphatidylinositol 3-kinase pathway. *Blood* **100**, 3087-3094.

Takahashi, K. and Yamanaka, S. (2006). Induction of pluripotent stem cells from mouse embryonic and adult fibroblast cultures by defined factors. *Cell* **126**, 663-676.

Tateishi, K., Ashihara, E., Honsho, S., Takehara, N., Nomura, T., Takahashi, T., Ueyama, T., Yamagishi, M., Yaku, H., Matsubara, H. et al. (2007). Human cardiac stem cells exhibit mesenchymal features and are maintained through Akt/GSK-3beta signaling. *Biochem. Biophys. Res. Commun.* **352**, 635-641.

Tomita, Y., Matsumura, K., Wakamatsu, Y., Matsuzaki, Y., Shibuya, I., Kawaguchi, H., Ieda, M., Kanakubo, S., Shimazaki, T., Ogawa, S. et al. (2005). Cardiac neural crest cells contribute to the dormant multipotent stem cell in the mammalian heart. *J. Cell Biol.* **170**, 1135-1146.

Tsai, M. S., Hwang, S. M., Tsai, Y. L., Cheng, F. C., Lee, J. L. and Chang, Y. J. (2006). Clonal amniotic fluid-derived stem cells express characteristics of both mesenchymal and neural stem cells. *Biol. Reprod.* **74**, 545-551.

Urbanek, K., Quaini, F., Tasca, G., Torella, D., Castaldo, C., Nadal-Ginard, B., Leri, A., Kajstura, J., Quaini, E. and Anversa, P. (2003). Intense myocyte formation from cardiac stem cells in human cardiac hypertrophy. *Proc. Natl. Acad. Sci. USA* **100**, 10440-10445.

Urbanek, K., Rota, M., Cascapera, S., Bearzi, C., Nascimbene, A., De Angelis, A., Hosoda, T., Chimenti, S., Baker, M., Limana, F. et al. (2005a). Cardiac stem cells possess growth factor-receptor systems that after activation regenerate the infarcted myocardium, improving ventricular function and long-term survival. *Circ. Res.* **97**, 663-673.

Urbanek, K., Torella, D., Sheikh, F., De Angelis, A., Nurzynska, D., Silvestri, F., Beltrami, C. A., Bussani, R., Beltrami, A. P., Quaini, F. et al. (2005b). Myocardial regeneration by activation of multipotent cardiac stem cells in ischemic heart failure. *Proc. Natl. Acad. Sci. USA* **102**, 8692-8697.

Urbanek, K., Cesselli, D., Rota, M., Nascimbene, A., De Angelis, A., Hosoda, T., Bearzi, C., Boni, A., Bolli, R., Kajstura, J. et al. (2006). Stem cell niches in the adult mouse heart. *Proc. Natl. Acad. Sci. USA* **103**, 9226-9231.

Wessels, A. and Perez-Pomares, J. M. (2004). The epicardium and epicardially derived cells (EPDCs) as cardiac stem cells. *Anat. Rec. A Discov. Mol. Cell. Evol. Biol.* **276**, 43-57.

Wu, S. M., Fujiwara, Y., Cibulsky, S. M., Clapham, D. E., Lien, C. L., Schultheiss, T. M. and Orkin, S. H. (2006). Developmental origin of a bipotential myocardial and smooth muscle cell precursor in the Mammalian heart. *Cell* **127**, 1137-1150.

Yang, Z., Berr, S. S., Gilson, W. D., Toufektsian, M. C. and French, B. A. (2004). Simultaneous evaluation of infarct size and cardiac function in intact mice by contrast-enhanced cardiac magnetic resonance imaging reveals contractile dysfunction in noninfarcted regions early after myocardial infarction. *Circulation* **109**, 1161-1167.

Yoon, Y. S., Wecker, A., Heyd, L., Park, J. S., Tkebuchava, T., Kusano, K., Hanley, A., Scadova, H., Qin, G., Cha, D. H. et al. (2005). Clonally expanded novel multipotent stem cells from human bone marrow regenerate myocardium after myocardial infarction. *J. Clin. Invest.* **115**, 326-338.

Available online at www.sciencedirect.com
ScienceDirect
Biochemical and Biophysical Research Communications 352 (2007) 635–641
BBRC
www.elsevier.com/locate/ybbrc

Human cardiac stem cells exhibit mesenchymal features and are maintained through Akt/GSK-3β signaling

Kento Tateishi [a,b], Eishi Ashihara [a], Shoken Honsho [a,b], Naofumi Takehara [a], Tetsuya Nomura [a,b], Tomosaburo Takahashi [b], Tomomi Ueyama [a], Masaaki Yamagishi [c], Hitoshi Yaku [c], Hiroaki Matsubara [a,b,*], Hidemasa Oh [a,*]

[a] *Department of Experimental Therapeutics, Translational Research Center, Kyoto University Hospital, Kyoto 606-8507, Japan*
[b] *Department of Cardiovascular Medicine, Kyoto Prefectural University School of Medicine, Kyoto 602-8566, Japan*
[c] *Department of Cardiovascular Surgery, Kyoto Prefectural University School of Medicine, Kyoto 602-8566, Japan*

Received 9 November 2006
Available online 27 November 2006

Abstract

Recent evidence suggested that human cardiac stem cells (hCSCs) may have the clinical application for cardiac repair; however, their characteristics and the regulatory mechanisms of their growth have not been fully investigated. Here, we show the novel property of hCSCs with respect to their origin and tissue distribution in human heart, and demonstrate the signaling pathway that regulates their growth and survival. Telomerase-active hCSCs were predominantly present in the right atrium and outflow tract of the heart (infant > adult) and had a mesenchymal cell-like phenotype. These hCSCs expressed the embryonic stem cell markers and differentiated into cardiomyocytes to support cardiac function when transplanted them into ischemic myocardium. Inhibition of Akt pathway impaired the hCSC proliferation and induced apoptosis, whereas inhibition of glycogen synthase kinase-3 (GSK-3) enhanced their growth and survival. We conclude that hCSCs exhibit mesenchymal features and that Akt/GSK-3β may be crucial modulators for hCSC maintenance in human heart.

Keywords: Cardiac stem cells; Mesenchymal cells; Proliferation; Survival; Akt/GSK-3β

The postmitotic heart was shown to exhibit a previously unappreciated self-renewing phenotype, in which primitive cells proliferated and differentiated into specific progeny under acute or chronic workloads [1,2]. Recent studies have challenged this paradigm and shown the existence of intrinsic cardiac stem or progenitor cells in the mammalian heart [3–5]. CSCs expressing c-kit were clonogenic and multipotent [4,6], and were also able to be isolated from human heart in the floating culture system [7]. Furthermore, hCSCs were reported to be activated in response to myocardial ischemia and increased workload [8,9]. These cells have a significant impact on future clinical application to treat patients with heart failure. However, it is necessary to further examine the property and regulatory mechanism of hCSC growth to obtain a sufficient number of stem cells from a small amount of tissue samples to achieve an efficient regenerative-therapy.

Recent reports have suggested that bone marrow-derived mesenchymal stem cells (MSCs) enhanced with Akt, a serine/threonine protein kinase, can repair infarcted myocardium, prevent remodeling, and normalize cardiac performance through the prevention of apoptosis as well as a paracrine effect on resident cells [10,11]. Recently, insulin-like growth factor-1 (IGF1) has been shown to maintain murine CSC (mCSC) viability and growth through activation of Akt [12,13]; however, the downstream signals of

* Corresponding authors. Fax: +81 75 751 4741.
E-mail addresses: matsubah@koto.kpu-m.ac.jp (H. Matsubara), hidemasa@kuhp.kyoto-u.ac.jp (H. Oh).

0006-291X/$ - see front matter © 2006 Elsevier Inc. All rights reserved.
doi:10.1016/j.bbrc.2006.11.096

Akt pathway in hCSC growth remain to be investigated. In the present study, we characterized the property of hCSCs and clarified the role of Akt/GSK-3β signaling pathway in hCSC growth and survival. These results suggest that pharmacological inhibition of GSK-3β may have practical application in hCSC transplantation therapy in human heart failure.

Materials and methods

Tissue samples. The heart samples were obtained from 18 patients undergone cardiac surgery (9 males and 9 females aged from 9 days to 77 years old) in confirmation with the guidelines of the Kyoto University Hospital and Ministry of Education, Culture, Sports, Science, and Technology, Japan.

Isolation of hCSCs. The heart samples were excised, minced, and digested with 0.4% type II collagenase and 0.01% DNAse. Obtained cells were then plated at 20 cells/μl in ultra-low culture dishes to generate cardiospheres with growth medium containing DMEM/F12, 5% FBS, 20 ng/ml EGF (Sigma), and 40 ng/ml bFGF (Promega). For the analyses described below, generated cardiospheres were dissected into single cells to obtain hCSCs by exposure to a 0.05% Trypsin/EDTA solution.

hCSC differentiation. For cardiac differentiation, hCSCs were cultured in differentiation medium containing 10% FBS, insulin-transferrin-selenium, and 10 nM dexamethasone. Differentiation medium containing DMEM/F12 supplemented with 10 ng/ml VEGF or 50 ng/ml PDGF-BB (R&D Systems) and 10% FBS was used to induce endothelial or smooth muscle cell differentiation, respectively. For the assay of cell proliferation and survival, specific inhibitors for Akt and GSK-3 (BIO) were purchased from Calbiochem.

FACS analysis. hCSCs were labeled with the following antibodies; phycoerythrin-conjugated antibodies against c-kit, CD45, CD34, CD31, CD90, CD29, CD73, CD71 (BD Biosciences), CD105 (Ancell Corp), and Stro-1 (R&D Systems). Cell events were collected by FACS Calibur flow cytometer and data were analyzed by Cell Quest (BD Biosciences).

RT-PCR and telomerase activity. Total RNA was extracted from cells using TRIzol and RT-PCR was performed with a SuperScript III First-Strand Synthesis System. The primer sequences are available upon request. Telomerase activity was measured with a TRAP assay kit, TRAPEZE (Chemicon).

Immunochemistry. Fixed cells and sections were stained with primary antibodies against cardiac troponin-I (Scripps), CD31, Ki67 (DAKO), α-SMA, connexin 43 (Sigma), collagen typeI (LSL), vimentin, and human nuclei (Chemicon). Secondary antibodies were conjugated to Alexa 488 and Alexa 555, and nuclei were visualized with 4′,6-diamidino-2-phenylindole (DAPI). Apoptotic hCSCs were evaluated by TUNEL assay with ApopTag kit (Chemicon). Images were captured with a BZ-8000 (Keyence) and IX71 (Olympus Corporation).

Myocardial infarction (MI) and cell grafting. MI was created in 12- to 24-week-old NOD/*scid* mice (Jackson Laboratories) in accordance with the animal care and use guidelines at Kyoto University Hospital. MI was induced by ligation of the left anterior descending coronary artery. One hour after MI, 3×10^5 hCSCs were injected into two sites of the infarcted border zone. In the control group, mice were sham-operated on receiving a thoracotomy but no ligation of coronary artery.

Echocardiography. Two-dimensional and M-mode recordings (Sonos 5500, PHILIPS) were obtained from the short-axis view at the midpapillary muscle level.

Western blotting. Cell lysates were extracted with lysis buffer containing 50 mM Tris–HCl (pH 7.4), 150 mM NaCl, 0.25% sodium deoxycholate, 1 mM EDTA, 1% Nonidet P-40, 1 mM PMSF, 1× protease inhibitor, 1 mM Na_3VO_4, and 1 mM NaF. Transferred membranes were incubated with primary antibodies against GSK-3β (BD Biosciences), phospho-GSK-3β (Ser9), phospho-Akt (S473), and Akt (Cell Signaling). Horseradish peroxidase (HRP)-conjugated anti-mouse IgG and HRP-conjugated anti-rabbit IgG were used as secondary antibodies.

Statistics. Data are means ± SE, and were analyzed by ANOVA and Scheffe's test, using a significance level of $p < 0.05$ (StatView).

Results

Identification and distribution of hCSCs in human heart

To characterize the hCSCs in human heart, primary heart-derived cells from patients were cultured at low density with low serum condition in a floating culture system using a modification of the method previously reported [7]. At day-14, spherical colonies were generated at a frequency of 63.1 ± 16.5 spheres per 200,000 viable cells (Fig. 1A). The initial yield of digested cells was proportional to the number of spheres, and the number of isolated cells was significantly increased in heart tissues from the right atrium (RA) and outflow tract (OFT) than in tissue from the left ventricle (LV) (Fig. 1B). Moreover, the isolated cells were 5-fold greater and had higher telomerase activity in the infant heart than the adult heart (Fig. 1C and D).

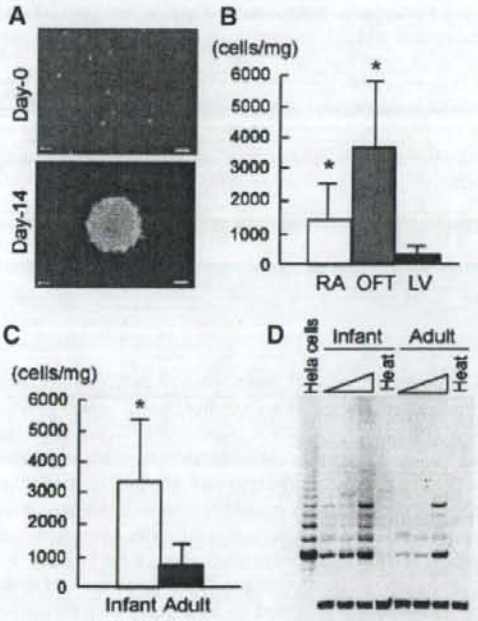

Fig. 1. Isolation and distribution of hCSCs. (A) Generation of cardiosphere from human heart. Bars, 20 μm. (B, C) The initial progenitor cell number harvested by primary isolation as indicated. Total yield was corrected by tissue weight (mg). Distribution of hCSCs corresponding to the parts of the heart (B) or the patients' age (C). $^*p < 0.05$ versus LV in (B); $^*p < 0.01$ versus adult in (C). (D) Telomerase activity in hCSCs. Threefold serial dilutions of hCSCs isolated from infant and adult hearts were treated with or without heat and used as templates. HeLa cells were used as a positive control ($n = 3$).

hCSCs exhibit mesenchymal features

Immunophenotyping revealed that hCSCs rarely expressed c-kit and did not express the hematopoietic and endothelial progenitor cell-specific surface antigens: CD45, CD34, and CD31, while they were positive for typical MSC surface antigens: CD105, CD90, CD29, CD73, CD71, and Stro-1 (Fig. 2A) [14,15]. Human cardiospheres also expressed both vimentin and collagen type 1 (Fig. 2B), and had a spindle shaped morphology in attached cell-culture experiments (Fig. 2C). RT-PCR showed that hCSCs expressed ATP-binding cassette transporter subfamily G member 2 (ABCG2), which was associated with Hoechst's efflux properties prerequisite for the side population cells [16]. Human cardiospheres also expressed Rex1, Nanog, and Sox2, although Oct4 was not detectable (Fig. 2D), suggesting that hCSCs express the embryonic stem cell markers and contain the mesenchymal cell-like population.

hCSCs give rise to cardiovascular lineages in vitro and in vivo

To determine the differentiation potential of hCSCs *in vitro*, hCSCs were cultured in differentiation medium. Immunostaining showed that hCSCs gave rise to smooth muscle cells, endothelial cells, and cardiomyocytes co-expressing connexin-43 (Fig. 3A). Furthermore, cardiac-specific transcriptional factors such as Nkx2.5 and GATA4, ANP, and structural genes, including α-cardiac-actin, cardiac troponin-T, MLC2a, MLC2v, α-MHC, and β-MHC, were detected in the differentiated cardiomyocytes by RT-PCR (Fig. 3B).

To investigate the regenerative potential of hCSCs *in vivo*, we performed cell transplantation into MI using NOD/*scid* mice. The injected cells formed a successful engraftment within the border and infarcted regions. The differentiation of hCSCs into the cardiovascular-lineage cells was verified by the presence of smooth muscle cells, endothelial cells, and cardiomyocytes, colocalized with human nuclei (Fig. 3C). Capillary density was also increased in the implanted hearts compared with the PBS-treated hearts (Fig. 3D).

After the transplantation of hCSCs, cardiac function was analyzed by echocardiography (Fig. 3E). In PBS-treated mice, the ejection fraction (EF) and fractional shortening (FS) were significantly decreased (EF: $81.5 \pm 2.0\%$ to $46 \pm 2.0\%$, $p < 0.01$; FS: $43.7 \pm 2.0\%$ to $20.2 \pm 1.0\%$, $p < 0.01$), and LV diastolic dimension (Dd) was expanded (35.2 ± 2.0 to 47.0 ± 3.0 mm, $p < 0.01$) at day-14 after MI compared with baseline. In contrast, the implantation of hCSCs effectively ameliorated the cardiac dysfunction (EF: $46 \pm 2.0\%$ vs $58 \pm 2.0\%$, $p < 0.01$; FS: $20.2 \pm 1.0\%$ vs $26.2 \pm 2.0\%$, $p < 0.01$) and reduced LV dilatation (Dd: $47.0 \pm 3.0\%$ vs $40.7 \pm 2.0\%$, $p < 0.01$) compared with PBS-injected mice. These parameters showed that the

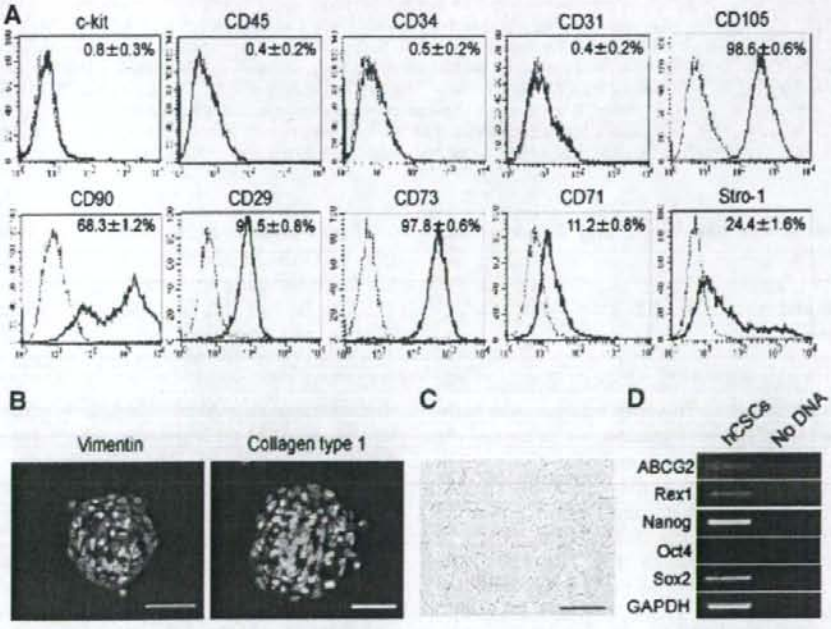

Fig. 2. Characterization of hCSCs. (A) FACS analysis of hCSCs. Black line, control IgG; red line, corresponding antibody ($n = 3$). (B) Immunostaining of human cardiospheres. Red signals show the expression of vimentin (left) and collagen type1 (right). Scale bars, 50 μm. (C) Phase contrast image of hCSCs in attached cell-culture. Scale bars, 100 μm. (D) Gene expression profile by RT-PCR examined in hCSCs. No DNA template was used as a negative control ($n = 6$).

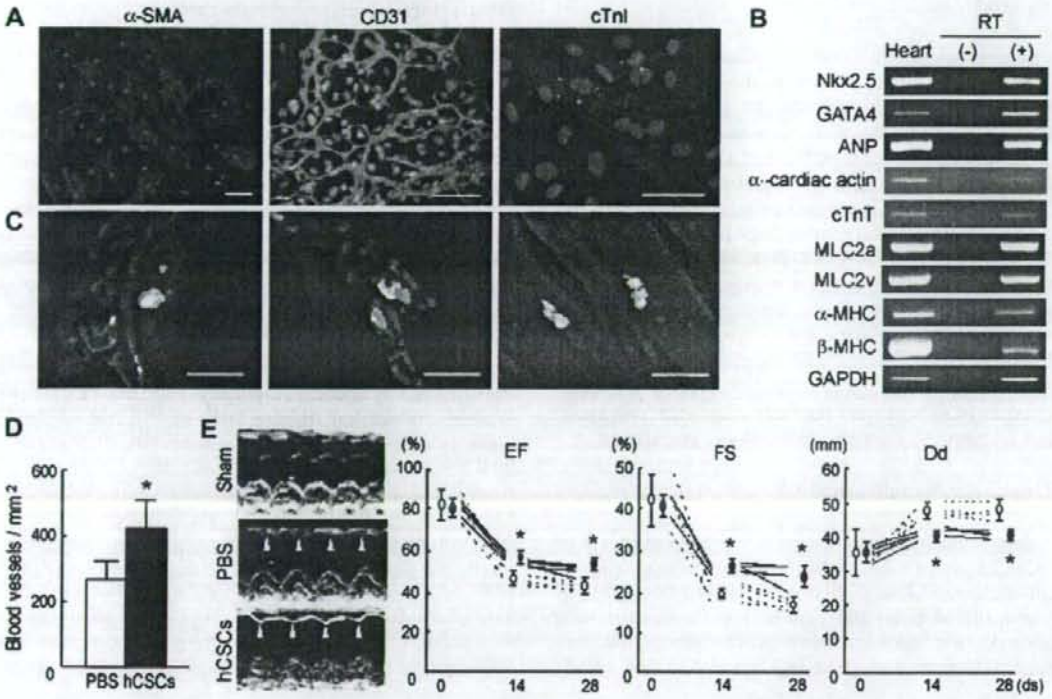

Fig. 3. Functional differentiation of hCSCs *in vitro* and *in vivo*. (A) *In vitro* differentiation of hCSCs into smooth muscle cells (left: α-SMA, red), endothelial cells (middle: CD31, green), and cardiomyocytes (right: cardiac troponin-I, red; connexin-43, yelow). DAPI, blue. (B) RT-PCR shows cardiac differentiation of hCSCs. Heart tissue was used as positive control ($n = 3$). (C) *In vivo* differentiation of hCSCs. Smooth muscle cells (left: α-SMA, red), endothelial cells (middle: CD31, red), and cardiomyocytes (right: cardiac troponin-I, red), counterstained with human nuclei (green) are shown. DAPI, blue ($n = 4$). (D) Capillary density was assessed by CD31 immunohistochemistry in the border zone. $^*p < 0.01$ versus PBS treated mice. (E) Serial assessment of cardiac function by echocardiography. Representative M-mode images of sham-operated, PBS-injected, and hCSC-transplantated hearts at 28 days after MI. Closed circles, hCSC transplanted hearts; open circles, PBS-injected hearts ($n = 8$). Arrowheads indicate significantly improved anterior wall movement on stem cell implantation. $^*p < 0.01$ versus PBS-treated mice. Scale bars, 50 μm in (A); 20 μm in (C).

significant recovery was observed 2 and 4 weeks after hCSC implantation.

The proliferation and survival of hCSCs depend on Akt/GSK-3β pathway

Akt pathway plays a crucial role to mediate the proliferation activity in mCSCs [13]. To verify whether Akt pathway was involved in hCSC proliferation, we examined the activation of Akt in hCSCs and found that EGF/bFGF treatment of hCSCs caused a rapid activation of Akt (Fig. 4A) and also augmented sustained phosphorylation of GSK-3β, which is one of the downstream targets of Akt, to inactivate GSK-3β function (Fig. 4B). The EGF/bFGF-induced activation of Akt in hCSCs was inhibited by Akt inhibitor, Akt-I, in a dose-dependent manner (Fig. 4C). In contrast, the levels of phosphorylated GSK-3β (inactive form of GSK-3β) could be enhanced by the treatment of 10 nM GSK-3-inhibitor, BIO (Fig. 4D), as previously reported in renal epithelial cells [17].

If Akt mediates hCSC proliferation through the inhibition of GSK-3β, the pharmacological inhibition of Akt/GSK-3β signaling pathways may affect the growth of hCSCs. To test this hypothesis, the diameter of cardiospheres was measured in the presence or absence of 10 μM Akt-I or 10 nM BIO, the minimal doses needed to achieve an effect shown above (Fig. 4C and D). Our results demonstrated that Akt-I significantly decreased the diameter of EGF/bFGF-expanded cardiospheres (Fig. 4E), whereas addition of BIO significantly increased their growth at the range of sphere size more than 100 μm (Fig. 4F).

We next determined the underlying mechanisms by which Akt/GSK-3β pathway modulated sphere formation and growth of hCSCs. $TUNEL^+$ cells were significantly increased in cardiospheres treated with Akt-I compared with control, whereas BIO apparently reduced the number of $TUNEL^+$ cells (Fig. 4G). In contrast, Ki67-positive cells were apparently decreased in cardiospheres treated with Akt-I compared with control, whereas a significant

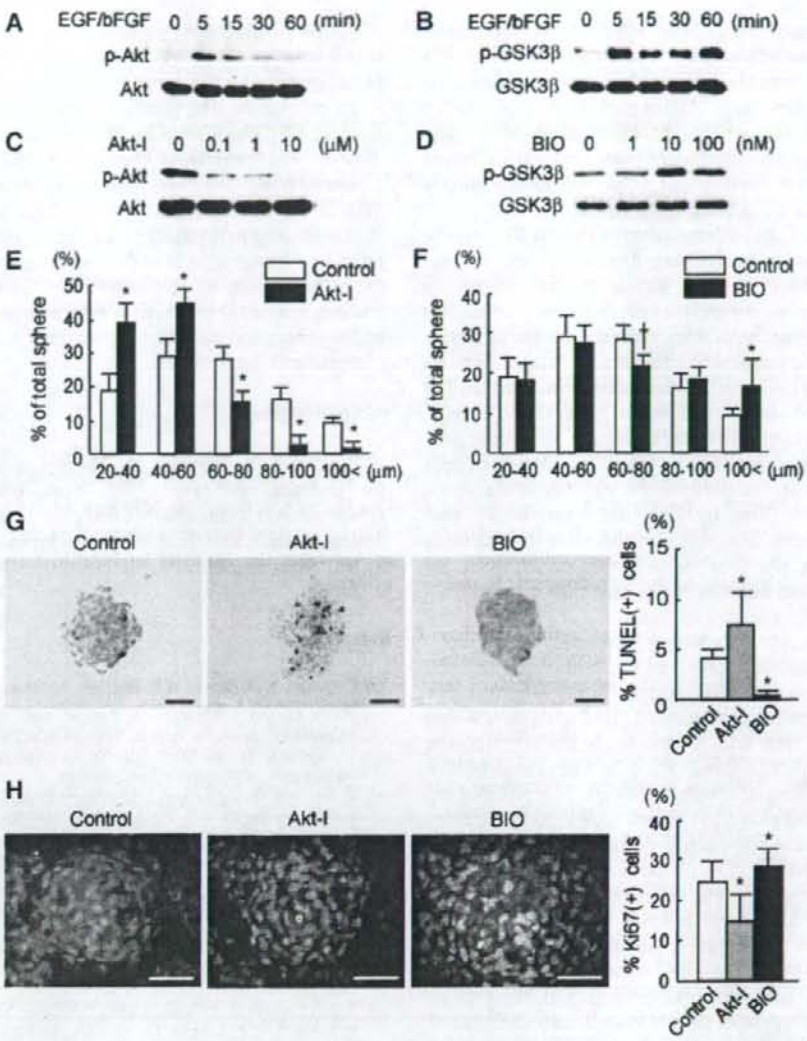

Fig. 4. Akt/GSK-3β signaling regulates the proliferation and survival of hCSCs. (A,B) Phosphorylation of Akt (A) and GSK-3β (B) induced by EGF/bFGF in hCSCs. After serum starvation for 2 h, hCSCs were treated with EGF/bFGF for the period of time indicated. (C) Activation of Akt induced by EGF/bFGF treatment for 5 min was abolished by the pretreatment of Akt-I for 4 h in a dose-dependent manner. (D) Phosphorylation of GSK-3β (inactive) induced by EGF/bFGF treatment for 5 min was enhanced by the pretreatment of 10 nM BIO for 4 h. (E,F) Size distribution of cardiospheres cultured in EGF/bFGF-containing medium in the presence of either 10 μM Akt-I (E), or 10 nM BIO (F) for 6 days ($n = 7$). $^{*}p < 0.01$ and $^{\dagger}p < 0.05$ versus DMSO control. (G,H) TUNEL assay (G) and Ki67 staining (H) of cardiospheres exposed to 10 μM Akt-I and 10 nM BIO. Ki67, red. DAPI, blue. $^{*}p < 0.01$ versus DMSO control ($n = 3$). Scale bars, 50 μm.

increase in the number of Ki67-positive cells was observed in cardiospheres exposed to BIO (Fig. 4H).

Discussion

Our present study provides the novel evidence that hCSCs exhibit a mesenchymal cell-like property and Akt/GSK-3β signaling is involved in their proliferation and survival. Furthermore, our study shows that hCSCs are predominantly present in the right atrium and outflow tract of the heart (more expressed in infant heart rather than adult heart).

A recent report has suggested that cellular aging induces a functional impairment of mCSC growth that may result from the reduction in Akt phosphorylation and telomerase inactivation [18]. Consistent with these data, we showed

here less telomerase activity in hCSCs from the adult heart than that from the infant heart. The abundance of hCSCs isolated from RA and OFT may reflect their specific distribution in the human heart. Although there is a possibility of bias caused by the patients' background, including disease, age, and sex, our results are consistent with a recent report showing that the stem cell niches are predominantly present in the atrium in the murine heart [19].

Messina et al. [7] have demonstrated that hCSCs can be isolated from human heart using floating culture system. We employed the essentially similar method to isolate hCSCs. However, in contrast to the previous report, we found that c-kit expression was extremely low in the isolated cells from both infant and adult hearts. Several reports demonstrated that c-kit expression was diminished on the lineage-committed cardiac progeny as observed in murine cardiac progenitor cells and cardioblasts [3,5,19]. It is possible that cardiospheres contain a mixed population of cells that, as in the niche, can promote the viability of c-kit progenitors and contribute to their proliferation [7]. Our observation suggest that mixed progenitor populations may exist during the process of lineage-commitment of hCSCs in the human heart as during hematopoietic homeostasis [20].

It is notable that hCSCs have a mesenchymal-like character. Mesenchymal stem cells were conventionally isolated from bone marrow and the presence in many tissues but not heart has recently been reported [21]. In the developing heart, the neural crest cells are known to migrate into the cardiac outflow tract to supply the cells from the primitive epicardial epithelium through a process of epithelial-to-mesenchymal transition [22]. These epicardially derived cells have a mesenchymal phenotype and stem cell property in human adult hearts [23]. Thus, it may be conceivable that hCSCs isolated from the human heart might be originated from the primitive epicardial epithelium.

The mechanism to regulate the proliferation and survival of stem cells has been examined. Akt is a nodal signaling kinase linked to both the proliferation and survival of somatic stem or progenitor cells in neural tissue and blood [24,25]. Our studies demonstrate that the proliferation of hCSCs appears to be dependent on the activation of Akt in response to EGF/bFGF stimulation. Furthermore, we have documented that inhibition of Akt pathway impairs cell growth and survival. Our observations are consistent with two independent studies demonstrating that *ex vivo* transduction of Akt prevents bone marrow-derived MSCs from the oxidative stress-induced apoptosis [10] and that the nuclear-targeting of Akt leads to an acceleration of mCSC expansion [13].

The novel finding we showed here that GSK-3β is also associated with the proliferation and survival of hCSCs may provide the new prospect for stem cell therapy. GSK-3β is one of the substrates of Akt and participates in regulating the cell cycle in various cell types [26]. We found that BIO stimulated the growth kinetics of hCSCs consistent with the observation seen in BIO-mediated proliferation of differentiated cardiomyocytes [27]. Thus, our findings suggest that Akt/GSK-3β pathway is crucial in hCSC growth and survival as well as mCSCs.

In conclusion, the present study demonstrates that the resident CSCs in human hearts have mesenchymal characteristics and proliferate through Akt/GSK-3β pathway. Understanding whether pharmacological inhibition of GSK3β by BIO may act through direct activation of the Wnt signaling pathway for stem cell maintenance [28] will provide a new insight into the signaling pathways required for hCSC expansion and engraftment *in vivo*. These novel findings may enable practical applications for establishing hCSC lines and provide an advanced cell therapy for patients with heart failure.

Acknowledgments

We thank Y. Yoshida, A. Kosugi, and M. Nishikawa for technical assistance. This work was supported by Grants-in-Aid from the Ministry of Education, Culture, Sports, Science and Technology of Japan, and by Grants-in-Aid from the Ministry of Health, Labor, and Welfare of Japan.

References

[1] F. Quaini, K. Urbanek, A.P. Beltrami, N. Finato, C.A. Beltrami, B. Nadal-Ginard, J. Kajstura, A. Leri, P. Anversa, Chimerism of the transplanted heart, N. Engl. J. Med. 346 (2002) 5–15.

[2] P. Anversa, B. Nadal-Ginard, Myocyte renewal and ventricular remodelling, Nature 415 (2002) 240–243.

[3] H. Oh, S.B. Bradfute, T.D. Gallardo, T. Nakamura, V. Gaussin, Y. Mishina, J. Pocius, L.H. Michael, R.R. Behringer, D.J. Garry, M.L. Entman, M.D. Schneider, Cardiac progenitor cells from adult myocardium: homing, differentiation, and fusion after infarction, Proc. Natl. Acad. Sci. USA 100 (2003) 12313–12318.

[4] A.P. Beltrami, L. Barlucchi, D. Torella, M. Baker, F. Limana, S. Chimenti, H. Kasahara, M. Rota, E. Musso, K. Urbanek, A. Leri, J. Kajstura, B. Nadal-Ginard, P. Anversa, Adult cardiac stem cells are multipotent and support myocardial regeneration, Cell 114 (2003) 763–776.

[5] K.L. Laugwitz, A. Moretti, J. Lam, P. Gruber, Y. Chen, S. Woodard, L.Z. Lin, C.L. Cai, M.M. Lu, M. Reth, O. Platoshyn, J.X. Yuan, S. Evans, K.R. Chien, Postnatal isl1+ cardioblasts enter fully differentiated cardiomyocyte lineages, Nature 433 (2005) 647–653.

[6] A. Linke, P. Muller, D. Nurzynska, C. Casarsa, D. Torella, A. Nascimbene, C. Castaldo, S. Cascapera, M. Bohm, F. Quaini, K. Urbanek, A. Leri, T.H. Hintze, J. Kajstura, P. Anversa, Stem cells in the dog heart are self-renewing, clonogenic, and multipotent and regenerate infarcted myocardium, improving cardiac function, Proc. Natl. Acad. Sci. USA 102 (2005) 8966–8971.

[7] E. Messina, L. De Angelis, G. Frati, S. Morrone, S. Chimenti, F. Fiordaliso, M. Salio, M. Battaglia, M.V. Latronico, M. Coletta, E. Vivarelli, L. Frati, G. Cossu, A. Giacomello, Isolation and expansion of adult cardiac stem cells from human and murine heart, Circ. Res. 95 (2004) 911–921.

[8] K. Urbanek, F. Quaini, G. Tasca, D. Torella, C. Castaldo, B. Nadal-Ginard, A. Leri, J. Kajstura, E. Quaini, P. Anversa, Intense myocyte formation from cardiac stem cells in human cardiac hypertrophy, Proc. Natl. Acad. Sci. USA 100 (2003) 10440–10445.

[9] K. Urbanek, D. Torella, F. Sheikh, A. De Angelis, D. Nurzynska, F. Silvestri, C.A. Beltrami, R. Bussani, A.P. Beltrami, F. Quaini, R. Bolli, A. Leri, J. Kajstura, P. Anversa, Myocardial regeneration by

activation of multipotent cardiac stem cells in ischemic heart failure, Proc. Natl. Acad. Sci. USA 102 (2005) 8692–8697.
[10] A.A. Mangi, N. Noiseux, D. Kong, H. He, M. Rezvani, J.S. Ingwall, V.J. Dzau, Mesenchymal stem cells modified with Akt prevent remodeling and restore performance of infarcted hearts, Nat. Med. 9 (2003) 1195–1201.
[11] M. Gnecchi, H. He, N. Noiseux, O.D. Liang, L. Zhang, F. Morello, H. Mu, L.G. Melo, R.E. Pratt, J.S. Ingwall, V.J. Dzau, Evidence supporting paracrine hypothesis for Akt-modified mesenchymal stem cell-mediated cardiac protection and functional improvement, FASEB J. 20 (2006) 661–669.
[12] K. Urbanek, M. Rota, S. Cascapera, C. Bearzi, A. Nascimbene, A. De Angelis, T. Hosoda, S. Chimenti, M. Baker, F. Limana, D. Nurzynska, D. Torella, F. Rotatori, R. Rastaldo, E. Musso, F. Quaini, A. Leri, J. Kajstura, P. Anversa, Cardiac stem cells possess growth factor-receptor systems that after activation regenerate the infarcted myocardium, improving ventricular function and long-term survival, Circ. Res. (2005).
[13] N. Gude, J. Muraski, M. Rubio, J. Kajstura, E. Schaefer, P. Anversa, M.A. Sussman, Akt promotes increased cardiomyocyte cycling and expansion of the cardiac progenitor cell population, Circ. Res. 99 (2006) 381–388.
[14] M.F. Pittenger, B.J. Martin, Mesenchymal stem cells and their potential as cardiac therapeutics, Circ. Res. 95 (2004) 9–20.
[15] Y. Sakaguchi, I. Sekiya, K. Yagishita, T. Muneta, Comparison of human stem cells derived from various mesenchymal tissues: superiority of synovium as a cell source, Arthritis Rheum. 52 (2005) 2521–2529.
[16] N. Kawanabe, K. Murakami, T. Takano-Yamamoto, The presence of ABCG2-dependent side population cells in human periodontal ligaments, Biochem. Biophys. Res. Commun. 344 (2006) 1278–1283.
[17] H. Wang, W.K. MacNaughton, Overexpressed beta-catenin blocks nitric oxide-induced apoptosis in colonic cancer cells, Cancer Res. 65 (2005) 8604–8607.
[18] D. Torella, M. Rota, D. Nurzynska, E. Musso, A. Monsen, I. Shiraishi, E. Zias, K. Walsh, A. Rosenzweig, M.A. Sussman, K. Urbanek, B. Nadal-Ginard, J. Kajstura, P. Anversa, A. Leri, Cardiac stem cell and myocyte aging, heart failure, and insulin-like growth factor-1 overexpression, Circ. Res. 94 (2004) 514–524.
[19] K. Urbanek, D. Cesselli, M. Rota, A. Nascimbene, A. De Angelis, T. Hosoda, C. Bearzi, A. Boni, R. Bolli, J. Kajstura, P. Anversa, A. Leri, Stem cell niches in the adult mouse heart, Proc. Natl. Acad. Sci. USA 103 (2006) 9226–9231.
[20] I.L. Weissman, Translating stem and progenitor cell biology to the clinic: barriers and opportunities, Science 287 (2000) 1442–1446.
[21] L. da Silva Meirelles, P.C. Chagastelles, N.B. Nardi, Mesenchymal stem cells reside in virtually all post-natal organs and tissues, J. Cell Sci. 119 (2006) 2204–2213.
[22] A. Wessels, J.M. Perez-Pomares, The epicardium and epicardially derived cells (EPDCs) as cardiac stem cells, Anat. Rec. A Discov. Mol. Cell. Evol. Biol. 276 (2004) 43–57.
[23] J. van Tuyn, D.E. Atsma, E.M. Winter, I. van der Velde-van Dijke, D.A. Pijnappels, N.A. Bax, S. Knaan-Shanzer, A.C. Gittenberger-de Groot, R.E. Poelmann, A. van der Laarse, E.E. van der Wall, M.J. Schalij, A.A. de Vries, Epicardial cells of human adults can undergo an epithelial-to-mesenchymal transition and obtain characteristics of smooth muscle cells in vitro, Stem Cells (2006).
[24] A.D. Sinor, L. Lillien, Akt-1 expression level regulates CNS precursors, J. Neurosci. 24 (2004) 8531–8541.
[25] F.H. Bahlmann, K. De Groot, J.M. Spandau, A.L. Landry, B. Hertel, T. Duckert, S.M. Boehm, J. Menne, H. Haller, D. Fliser, Erythropoietin regulates endothelial progenitor cells, Blood 103 (2004) 921–926.
[26] J. Liang, J.M. Slingerland, Multiple roles of the PI3K/PKB (Akt) pathway in cell cycle progression, Cell Cycle 2 (2003) 339–345.
[27] A.S. Tseng, F.B. Engel, M.T. Keating, The GSK-3 inhibitor BIO promotes proliferation in mammalian cardiomyocytes, Chem. Biol. 13 (2006) 957–963.
[28] N. Sato, L. Meijer, L. Skaltsounis, P. Greengard, A.H. Brivanlou, Maintenance of pluripotency in human and mouse embryonic stem cells through activation of Wnt signaling by a pharmacological GSK-3-specific inhibitor, Nat. Med. 10 (2004) 55–63.

Available online at www.sciencedirect.com
ScienceDirect
Biochemical and Biophysical Research Communications 352 (2007) 668–674
BBRC
www.elsevier.com/locate/ybbrc

Skeletal myosphere-derived progenitor cell transplantation promotes neovascularization in δ-sarcoglycan knockdown cardiomyopathy

Tetsuya Nomura [a,b], Eishi Ashihara [a], Kento Tateishi [a,b], Satoshi Asada [a,b], Tomomi Ueyama [a], Tomosaburo Takahashi [a,b], Hiroaki Matsubara [a,b], Hidemasa Oh [a,*]

[a] *Department of Experimental Therapeutics, Translational Research Center, Kyoto University Hospital, Kyoto 606-8507, Japan*
[b] *Department of Cardiovascular Medicine, Kyoto Prefectural University of Medicine, Kyoto 602-8566, Japan*

Received 10 November 2006
Available online 27 November 2006

Abstract

Bone marrow cells have been shown to contribute to neovascularization in ischemic hearts, whereas their impaired maturation to restore the δ-sarcoglycan (δ-SG) expression responsible for focal myocardial degeneration limits their utility to treat the pathogenesis of cardiomyopathy. Here, we report the isolation of multipotent progenitor cells from adult skeletal muscle, based on their ability to generate floating-myospheres. Myosphere-derived progenitor cells (MDPCs) are distinguishable from myogenic C2C12 cells and differentiate into vascular smooth muscle cells and mesenchymal progeny. The mutation in the δ-SG has been shown to develop vascular spasm to affect sarcolemma structure causing cardiomyopathy. We originally generated δ-SD knockdown (KD) mice and transplanted MDPCs into the hearts. MDPCs enhanced neoangiogenesis and restored δ-SG expression in impaired vasculatures through trans-differentiation, leading to improvement of cardiac function associated with paracrine effectors secretion. We propose that MDPCs may be the promising progenitor cells in skeletal muscle to treat δ-sarcoglycan complex mutant cardiomyopathy.

Keywords: Stem cells; Skeletal muscle; Angiogenesis; δ-Sarcoglycan; Mesenchymal cell

Satellite cells reside beneath the basal lamina of adult skeletal muscle and mediate the postnatal growth and regeneration of muscle [1]. However, a growing number of studies are reporting the isolation of stem cells from adult skeletal muscle tissue, distinct from or descendant from satellite cells [2,3]. Multipotent skeletal muscle-derived stem cells (MDSCs) were demonstrated to be composed of a subset of a Sca-1$^+$/CD34$^+$/CD45$^-$ cell population [4]. These cells exhibited greater neoangiogenesis as well as regeneration of cardiomyocytes when transplanted into myocardial infarction [5] or dystrophin-deficient mdx mice [6]. Myogenic and endothelial cell progenitors were also identified in the interstitial space of adult skeletal muscle. They were defined as a CD34$^+$/CD45$^-$ fraction, and differentiated into vascular endothelial cells and skeletal muscle fibers after transplantation into intact skeletal muscle [7].

To take advantage of potential therapeutic opportunities, as an easily accessible tissue source for autologous transplantation, we isolated the cells from adult skeletal muscle, based on the characteristics of adult stem cells having a distinct proliferative potential to form floating-spheres, termed myospheres [8]. Myosphere-derived progenitor cells (MDPCs) expressed phenotypic characteristics resembling microvascular pericytes [9] or mesenchymal stem cells (MSCs) [10]. When introduced into ischemic hearts, MSCs were shown to prevent deleterious remodeling and to improve cardiac function [11].

Cardiomyopathy is a multifactorial disease that includes both inherited and acquired forms and is one of the most

* Corresponding author. Fax: +81 75 751 4741.
E-mail address: hidemasa@kuhp.kyoto-u.ac.jp (H. Oh).

0006-291X/$ - see front matter © 2006 Elsevier Inc. All rights reserved.
doi:10.1016/j.bbrc.2006.11.097

common causes of chronic heart failure. A mutation in the δ-sarcoglycan (δ-SG) gene was demonstrated to lead to sarcoglycan complex disruption and dystrophic changes [12]. The absence of δ-SG specifically in vascular smooth muscle produced microinfarcts in the heart that resulted in cardiomyopathy characterized by irregularities of the coronary vasculature and focal degeneration [13]. In this study, we originally generated cardiomyopathy model by targeting δ-SG transcripts with efficient knockdown (KD) vector pDECAP-δ-SG [14]. δ-SG KD mice showed both less vascular density and reduced δ-SG expression in the hearts, resulted in cardiac dysfunction.

Bone marrow-derived side population (BM-SP) transplantation has been shown to engrafted into δ-SG-deficient hearts in the absence of restoration of δ-SG expression in cardiac muscle [15]. Therefore, the present study was designed to address the efficacy of cell therapy using MDPCs for the treatment of δ-SG KD-induced cardiac dysfunction. Our results showed that the implanted MDPCs not only regenerated new vessels but also promoted the secretion of paracrine effectors, thereby improving cardiac function.

Materials and methods

MDPC isolation. The primary hind limb muscle cells were isolated from 8-week-old C57BL/6J mice (Shimizu Laboratories Supplies) and green fluorescent protein (GFP) transgenic mice (generously donated by M. Okabe, Osaka University) using 470 U/ml collagenase type II (Worthington) for digestion. Cells were suspended in DMEM/F12 (Invitrogen) supplemented with B27, 20 ng/ml epidermal growth factor (EGF) (Sigma), and 40 ng/ml recombinant basic fibroblast growth factor (bFGF) (Promega). Cell suspensions were then cultured onto a non-coated dish at 20 cells/μl density over 7 days. Individual GFP^- spheres were transferred onto a 24-well fibronectin-coated plate in the growth medium composed of DMEM/F12, 2% fetal bovine serum (FBS), 20 ng/ml EGF, 10 ng/ml bFGF, and 10 ng/ml leukemia inhibitory factor (LIF) (Chemicon).

MDPC differentiation. Culture medium was replaced by specific medium composed of DMEM, 10% FBS, 0.5 mM isobutyl-methylxanthine, and 1 μM dexamethasone for adipogenic differentiation. Osteogenic differentiation was induced by treating cells with 250 ng/ml recombinant bone morphogenetic protein 2 (Sigma). Differentiation medium containing DMEM/F12 and 10% FBS supplemented with 10 ng/ml vascular endothelial growth factor or 50 ng/ml platelet-derived growth factor (R&D Systems) was used to induce endothelial or smooth muscle cell differentiation, respectively.

Generation of δ-SG KD mice. The plasmid to express first 498-bp coding region of δ-SG RNA was cloned by PCR using the full-length of δ-SG cDNA (generously donated by M. Imamura, National Institute of Neuroscience, Tokyo, Japan) [16]. A plasmid expressing the 498-bp of double-stranded δ-SG RNA was constructed into the KD vector, pDECAP (generously donated by S. Ishii, RIKEN Tsukuba Institute, Japan) [14], as an inverted repeat with a 12-bp spacer (CTCTCTGGTACC). The 2.2-kbp *Bgl*II–*Bam*HI fragment of pDECAP-δ-SG was released and injected into fertilized mouse oocytes.

RNA extraction and gene expression analysis. Total RNA was extracted using TRIzol reagent and first-strand cDNA was synthesized by SuperScript III kit (Invitrogen). Primers used were Sca-1-f: CTCTGAGGATG GACACTTCT, Sca-1-r: GGTCTGCAGGAGGACTGAGC; CD34-f: TTGACTTCTGCAACCACGGA, CD34-r: TAGATGGCAGGCTGG ACTTC; Pax7-f: GAAAGCCAAACACAGCATCGA, Pax7-r: ACCCTG ATGCATGGTTGATGG; MyoD-f: ACATAGACTTGACAGGCCC CGA, MyoD-r: AGACCTTCGATGTAGCGGATGG; Myogenin-f: TAC GTCCATCGTGGACAGCAT, Myogenin-r: TCAGCTAAATTCCCTC GCTGG; β-actin-f: GCTCGTCGTCGACAACGGCTC, β-actin-r: CAAACATGATCTGGGTCATCTTCTC; δ-SG-f: CCATGACCATC TGGATTCTCAAGG, δ-SG-r: GATGGCTTCCATATTGCCAGCTTC; and smooth muscle myosin heavy chain (Sm-MHC)-f: AGGAACTCC AAGCAAGTTGCAGG, Sm-MHC-r: CTGGAAGGAACAAATGAA GCCTCG. To evaluate hepatocyte growth factor (HGF) and stromal-cell-derived factor 1 (SDF-1) expression, cDNA was analyzed by kinetic real-time RT-PCR using the ABI Prism 7700 Sequence Detector system (Applied Biosystems) with Assay-on-Demand™ primer-probes sets. mRNA levels were expressed relative to an endogenous control (18S RNA).

Fluorescence activated cell sorting (FACS) analysis. Cells were stained with the following antibodies; FITC-conjugated antibodies against Sca-1, CD29, CD31, CD44, CD45, CD106, and CD117, PE-conjugated antibodies against CD34 and CD90 (BD Biosciences), and rat monoclonal anti-CD105 (Southern Biotechnology) followed by APC-labeled goat anti-rat IgG (BD Biosciences). Non-viable cells were stained with propidium iodide and 30,000 events were collected per sample by FACS Calibur flow cytometer (BD Biosciences). Gates were established by non-specific-Ig binding in each experiment.

Immunofluorescence. Specimens were fixed in 4% paraformaldehyde and stained with rat monoclonal anti-CD31 (BD Biosciences); rabbit polyclonal anti-type I collagen (LSL); mouse monoclonal antibodies against vimentin, Sm-MHC (DAKO), and δ-SG (Novocastra). Secondary antibodies were conjugated with Alexa 488 or Alexa 555, and nuclei were visualized using 4′,6-diamino-2-phenylindole (DAPI) (Invitrogen). Mouse monoclonal antibody against α-smooth muscle actin (α-SMA, Sigma) was conjugated with Cy3. M.O.M. Kit (Vector). Cells were labeled with 10 μM 5-bromo-2′-deoxyuridine (BrdU) solution for 1 h in culture and BrdU detection kit (Roche) was used according to the manufacturer's instruction. Images were captured with BZ-8000 (Keyence).

Oil red O and Alizarin red staining. Formalin-fixed cells were stained with 0.3% oil red O (Sigma) in 60% isopropanol for 30 min at room temperature. To stain calcium deposits, cells were covered with 2% alizarin red S solution (pH 4.2, Sigma) for 3 min.

Masson's trichrome and 5-bromo-4-chloro-3-indolyl-β-D-galactoside (X-gal) staining. Hearts from 28-week-old δ-SG KD mice were fixed with 10% formalin. Paraffin-embedded hearts were sectioned and stained with Masson's trichrome. Cell-implanted hearts were fixed by perfusion with 4% paraformaldehyde, and stained with the solution composed of 1 mg/ml X-gal (Invitrogen), 5 mM $K_4Fe(CN)_6$, 5 mM $K_3Fe(CN)_6$, 2 mM $MgCl_2$, 0.01% sodium deoxycholate, and 0.02% NP-40 for overnight.

Retroviral transduction. GP2-293 cells were co-transfected with the envelope vector pVSV-G and pMSCV-puro vectors using FuGENE6 (Roche). The medium supernatant was collected and centrifuged to concentrate viral stocks according to the manufacturer's instruction. MDPCs were infected with the retrovirus for 24 h, and the infected cells were selected with 2.5 μg/ml puromycin.

Surgical procedure. Anesthetized 28-week-old δ-SG KD mice ($n = 15$) were intubated and positive-pressure ventilation was maintained. A half million MDPCs diluted in 20 μl of phosphate-buffered saline (PBS) were directly transplanted into three distinct sites of myocardium. All experimental procedures and protocols using animals were approved by the Animal Care and Use Committee of Kyoto University.

Cardiac function. Echocardiograms were performed using SONOS 5500 and 15 MHz probe (PHILIPS). M-mode measurements of left ventricular end diastolic diameters (LVDd) were measured and used for the calculation of fractional shortening (FS) of the left ventricle (LV). As an index of LV diastolic function, transmitral early filling/atrial contraction ratio (E/A) values were determined from five independent measurements by using spectral Doppler traces.

Statistical analysis. All experiments were performed at least three times. Data were expressed as means ± standard error and analyzed by one-way ANOVA with post hoc analysis. A value of $p < 0.05$ was considered significant.

Results

Isolation and expansion of MDPCs

We isolated myospheres from adult skeletal muscle, based on the characteristics of adult stem cells having a distinct proliferative potential to form floating-spheres, by co-culturing the single cells from GFP transgenic and wild-type (WT) mice to exclude cell aggregation as confirmed by green mosaic fluorescence [17]. By day-7 in culture, spherical colonies composed of entirely GFP-positive or -negative cells had been formed ($0.11 \pm 0.03\%$ of initial cells, Fig. 1A). RT-PCR demonstrated that a single myosphere was positive for Sca-1 and CD34 but lacked essential myogenic transcription factors, including Pax7, MyoD, and Myogenin, which are typically present in myogenic C2C12 cells (Fig. 1B).

For MDPC expansion, individual GFP^- myospheres were transferred onto fibronectin-coated 24-well plates in the growth medium and the myospheres were allowed to attach on culture plates. Many cells migrated from the colony and were mitotically active cells as confirmed by BrdU incorporation (Fig. 1C). MDPCs continued to proliferate in the growth medium (Fig. 1D), and reached more than 120 population doublings as confirmed in three individual cell lines (Fig. 1E).

MDPCs have mesenchymal cell-like phenotype and differentiate into endothelial and vascular smooth muscle cells

FACS analysis showed that MDPCs expressed CD29, CD44, CD90, CD105, and CD106, a typical profile for mesenchymal cells. The lack of CD31, CD45, and CD117 indicated that the cells did not include endothelial or hematopoietic progenitors. Of note, Sca-1 and CD34 were highly expressed in MDPCs (Fig. 2A). To further address their mesenchymal-cell phenotype, undifferentiated MDPCs were stained for vimentin ($90.2 \pm 3.3\%$, Fig. 2B) and type I collagen ($87.4 \pm 6.9\%$, Fig. 2C). Induction of adipogenic- and osteogenic-lineage differentiation was examined in vitro. Accumulation of lipid vacuoles was clearly visualized by oil red O staining (Fig. 2D), and Alizarin red staining detected calcium deposits in osteogenic culture (Fig. 2E), indicating that MDPCs have a mesenchymal cell-like phenotype.

To determine the angiogenic potential of MDPCs, cells were cultured under specific inductions. Immunofluorescence analysis showed that MDPCs differentiated into $CD31^+$ vasculature (Fig. 2F) and Sm-MHC^+ smooth muscle cells in vitro (Fig. 2G).

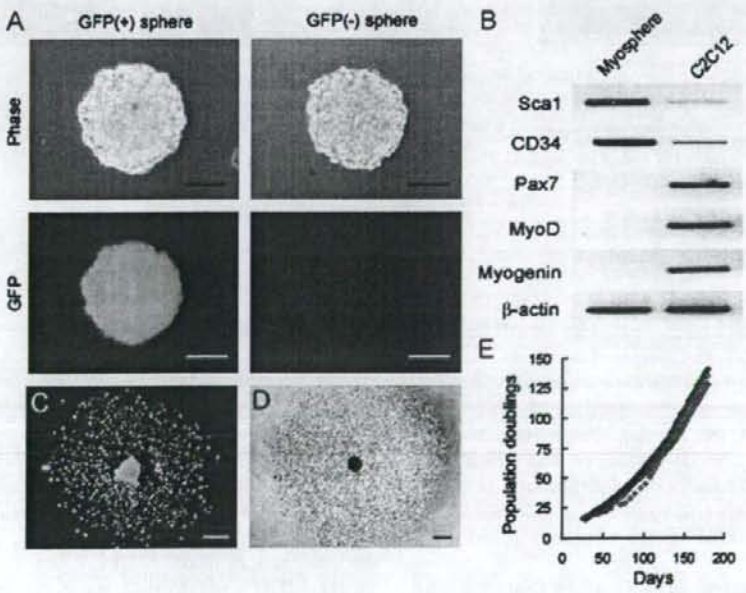

Fig. 1. Isolation and expansion of MDPCs. (A) Representative phase contrast and fluorescent images of myospheres generated from the mixed-cultures of single cells isolated from GFP transgenic (left panels) and WT mice (right panels). (B) RT-PCR analysis of Sca-1, CD34, and myogenic transcription factors. (C) MDPCs that migrated from single myosphere actively incorporated BrdU (green). DAPI (blue). (D) MDPCs propagated in the growth medium. (E) Growth kinetics of 3 independent cell lines in long-term culture. Scale bars represent 50 μm in (C) and (D), and 20 μm in (A).

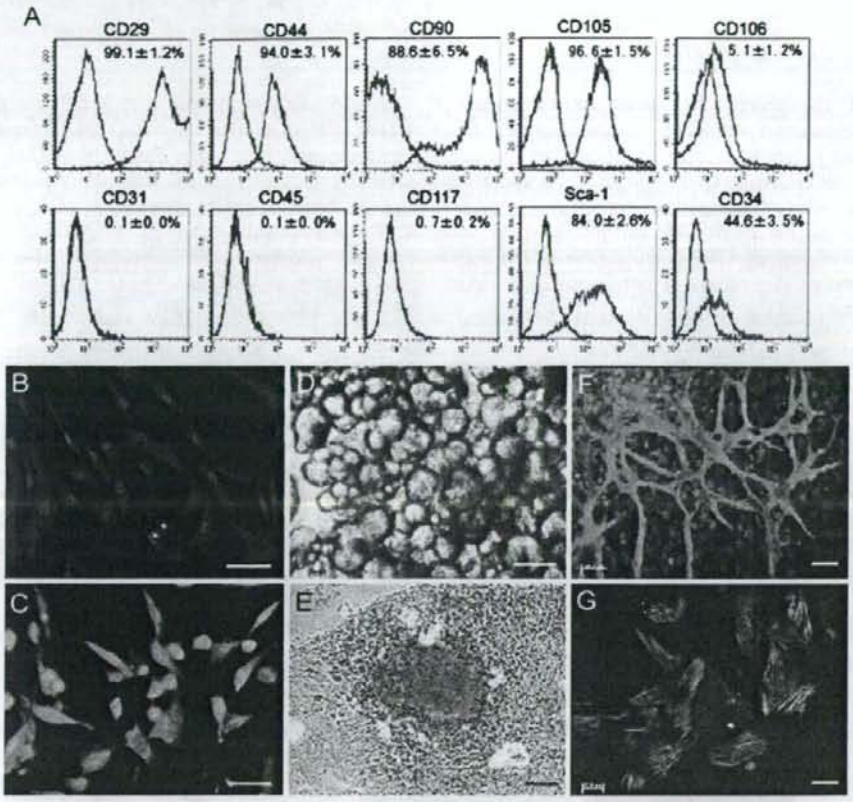

Fig. 2. MDPCs have mesenchymal cell-like phenotype and differentiate into endothelial and smooth muscle cells. (A) FACS analysis of MDPCs. Isotype controls were overlaid (blue lines) on each antigen tested (red lines). Immunostaining of mesenchymal markers on undifferentiated MDPCs. Vimentin (B, red) and type I collagen (C, green) are shown. DAPI (blue). Adipogenic- and osteogenic-inductions were verified by Oil red O (D, red) and Alizarin red (E, red), respectively. MDPCs were also induced into $CD31^+$ endothelial (F, green) and Sm-MHC^+ smooth muscle cells (G, red) by specific medium. DAPI (blue) Scale bars represent 50 μm in (E) and 20 μm in (B–D, F, and G).

MDPCs regenerate vascular smooth muscle cells with the restoration of δ-SG expression in vivo

We next generated δ-SG KD mice as a cardiomyopathy model by targeting δ-SG transcripts with an efficient KD vector, pDECAP-δ-SG [14]. Compared with non-transgenic littermates (NTG), the δ-SG expression on the membrane of cardiac muscle was disrupted in 28-week-old δ-SG KD mice (Fig. 3A left panels). The δ-SG expression along the vessels was also decreased, resulting in narrow vascular lumens with constrictive morphology (Fig. 3A middle panels). Masson's trichrome staining demonstrated extensive fibrosis surrounding the vessels (Fig. 3A right panels).

To determine whether MDPC transplantation can restore the δ-SG expression as well as regenerate the degenerated vessels in δ-SG KD hearts, a half million MDPCs transduced with a LacZ reporter gene were directly injected into three individual sites of myocardium. All transplanted hearts showed substantial $LacZ^+$ cell engraftment 4 weeks after implantation. $LacZ^+$ vascular smooth muscle cells could be readily detectable (Fig. 3B), and those were co-localized with δ-SG expression to regenerate new vessels (Fig. 3C arrows).

Transplantation of MDPCs improves cardiac function partially through the paracrine effectors production

We next asked whether MDPCs might restore δ-SG expression during differentiation process and found that MDPCs expressed δ-SG transcripts through smooth muscle cell lineage induction in vitro (Fig. 4A). A significant neoangiogenesis in the MDPC-injected area was observed in the MDPC-transplanted group compared with that in PBS-treated hearts (Fig. 4B). Cardiac function at baseline of δ-SG KD and NTG littermates was analyzed by echocardiography and showed a significant increase in LVDd and impaired systolic and diastolic functions in δ-SG KD